

Pacific Northwest National Laboratory

Operated by Battelle for the
U.S. Department of Energy

Self-Assembled Monolayers on Mesoporous Support (SAMMS) Technology for Contaminant Removal and Stabilization

Pacific Northwest National Laboratory, Richland, Washington

J. Liu
G. E. Fryxell
S. V. Mattigod

M. Gong
Z. Nie

Ferro Corp., Cincinnati, Ohio

X. Feng

University of California, Berkeley, California

K. N. Raymond

September 1998

RECEIVED
OCT 13 1998
OSTI

DISTRIBUTION OF THIS DOCUMENT IS UNLIMITED

MASTER

Prepared for the U.S. Department of Energy
under Contract DE-AC06-76RLO 1830

DISCLAIMER

This report was prepared as an account of work sponsored by an agency of the United States Government. Neither the United States Government nor any agency thereof, nor Battelle Memorial Institute, nor any of their employees, makes any warranty, expressed or implied, or assumes any legal liability or responsibility for the accuracy, completeness, or usefulness of any information, apparatus, product, or process disclosed, or represents that its use would not infringe privately owned rights. Reference herein to any specific commercial product, process, or service by trade name, trademark, manufacturer, or otherwise does not necessarily constitute or imply its endorsement, recommendation, or favoring by the United States Government or any agency thereof, or Battelle Memorial Institute. The views and opinions of authors expressed herein do not necessarily state or reflect those of the United States Government or any agency thereof.

PACIFIC NORTHWEST NATIONAL LABORATORY
operated by
BATTELLE MEMORIAL INSTITUTE
for the
UNITED STATES DEPARTMENT OF ENERGY
under Contract DE-AC06-76RLO 1830

Printed in the United States of America

Available to DOE and DOE contractors from the
Office of Scientific and Technical Information, P.O. Box 62, Oak Ridge, TN 37831;
prices available from (615) 576-8401.

Available to the public from the National Technical Information Service,
U.S. Department of Commerce, 5285 Port Royal Rd., Springfield, VA 22161

DISCLAIMER

Portions of this document may be illegible electronic image products. Images are produced from the best available original document.

Self-Assembled Monolayers on Mesoporous Support (SAMMS) Technology for Contaminant Removal and Stabilization

Pacific Northwest National Laboratory, Richland, Washington

J. Liu

M. Gong

G. E. Fryxell

Z. Nie

S. V. Mattigod

Ferro Corp., Cincinnati, Ohio

X. Feng

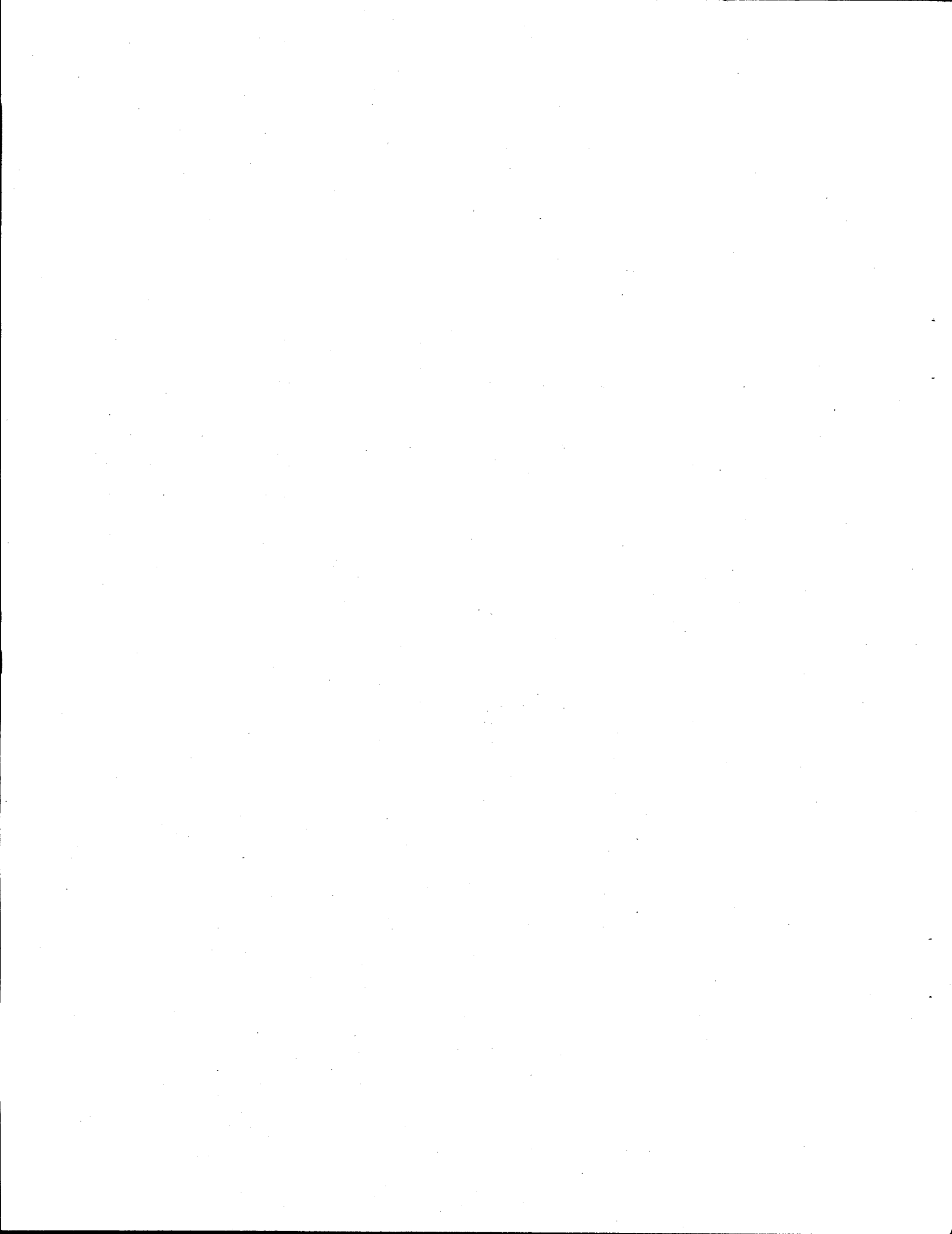
University of California, Berkeley, California

K. N. Raymond

September 1998

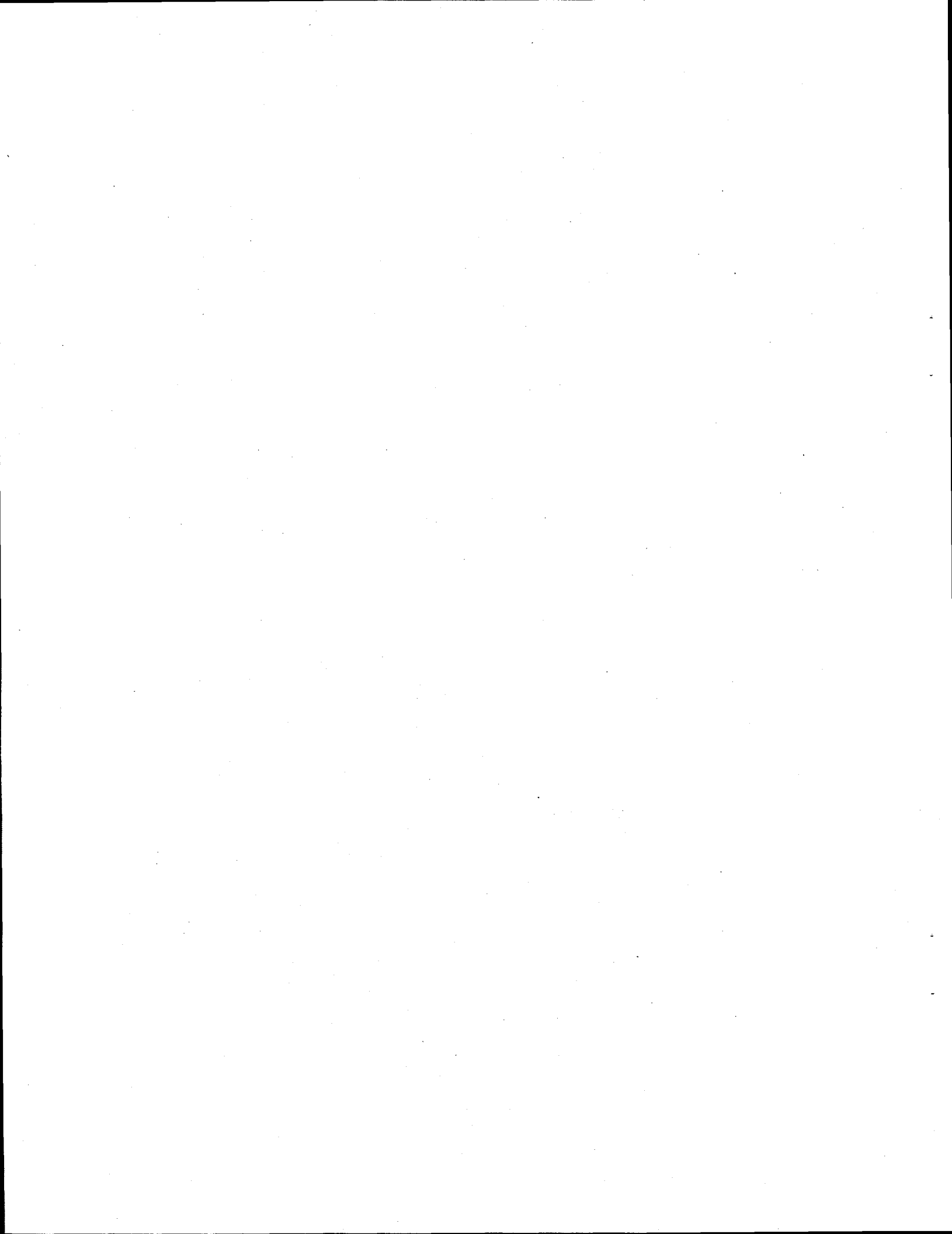
Prepared for the U.S. Department of Energy
under Contract DE-AC06-76RLO 1830

Pacific Northwest National Laboratory
Richland, Washington 99352



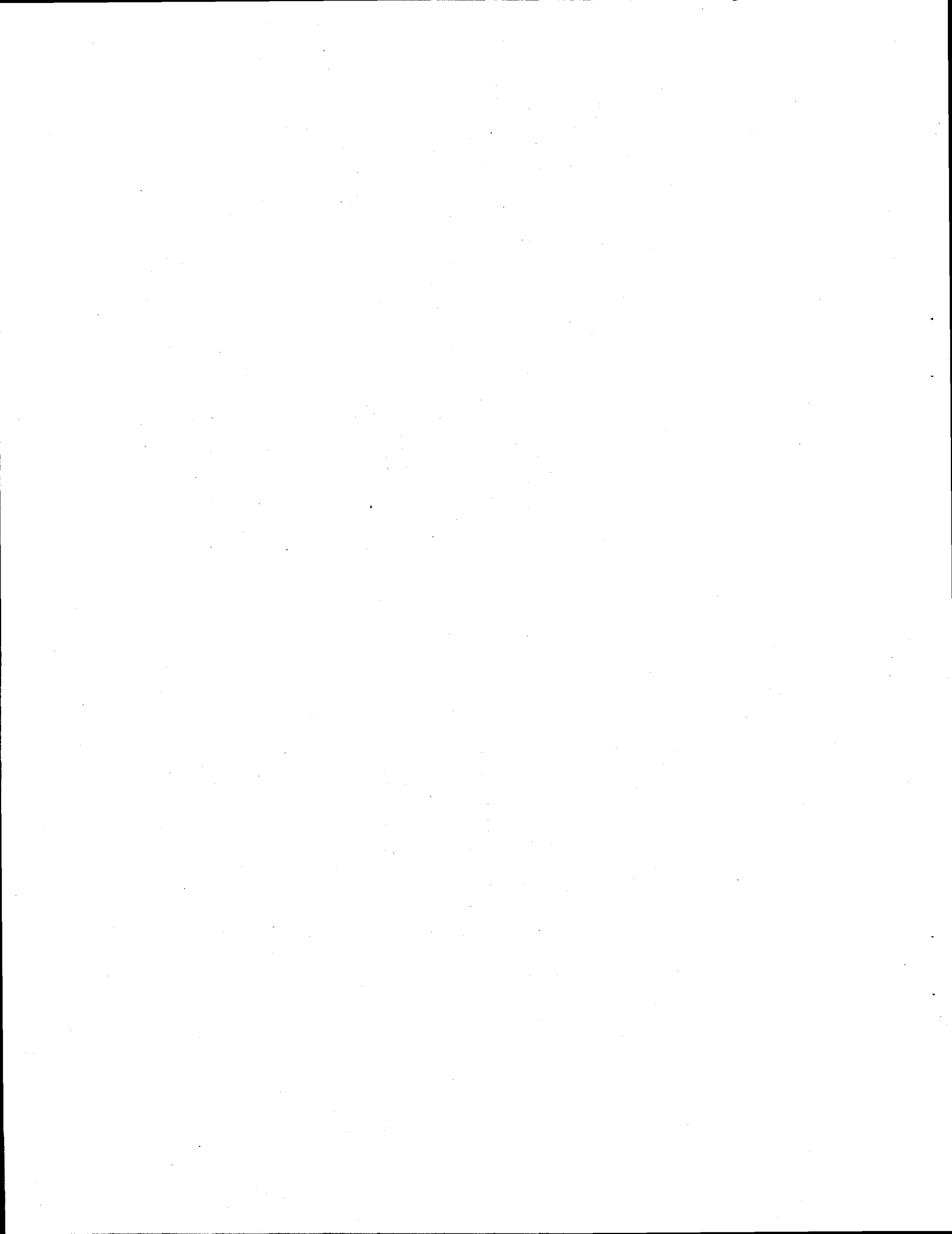
Summary

A study of mercury-adsorption kinetics showed that at all pH values (3, 5, 7 and 9), the adsorption by thiol-SAMMS occurred very rapidly (~ 82 to 95% of total mercury adsorption occurred within the first 5 min). The adsorption equilibrium in all cases was attained within ~4 h. At fixed solid:solution ratio, the mercury-loading density on thiol-SAMMS increased with decreasing iodide concentrations. The highest mercury loading of ~270 mg/g of thiol-SAMMS was observed at an iodide concentration of ~90 mmol/L. Calculated free energy of adsorption value showed that Hg^{2+} ion has high affinity for thiol-groups. This strong adsorption affinity is typical of soft-cation/soft-base interaction. Very high distribution coefficient values (K_d , 1.29×10^5 mL/g to $>2.64 \times 10^8$ mL/g) indicated that thiol-SAMMS adsorbs mercury from $\text{KI-K}_2\text{SO}_4$ solutions with very high specificity. Data from an adsorption experiment with model organic ligands indicated that ammonia, cyanide, and EDTA had no noticeable effect on mercury adsorption by thiol-SAMMS. In the presence of a strongly complexing natural ligand (fulvate), thiol-SAMMS removed ~92 to 99% of mercury in solution. Actinide adsorption experiments showed that 1,2-HOPO-SAMMS had very high affinity for (K_d : 1.9×10^5 to 4.43×10^5 mL/g) for Am(III), a high affinity (K_d : 3.3×10^3 to 3.6×10^3 mL/g) for Np(V), and moderate affinities (K_d : 160 to 840 mL/g) for Th(IV) and U(VI). Thiol-SAMMS also showed very high affinity (K_d : $>1.0 \times 10^4$ mL/g) for Pu(VI) and high affinities (K_d : 4.0×10^3 to 6.2×10^3 mL/g) for Am(III) and Pu(IV) (K_d : 1.7×10^3 mL/g). The 1,2-HOPO-SAMMS, and thiol-SAMMS were significantly more effective than resin-forms for adsorbing actinides. Results from an adsorption study conducted with selected transition metal cations indicated that thiol-SAMMS has high affinities for adsorbing soft cations such as Ag, Cd, Cu(II), Cr(III), and Pb. These data confirmed the high specificity of soft-base thiol groups for adsorbing soft acid cations. Due to its high specificity, thiol-SAMMS can selectively adsorb and separate Ag, Cd, Cu(II), Cr(III), Hg, and Pb from solutions containing alkali and alkaline earth cations.



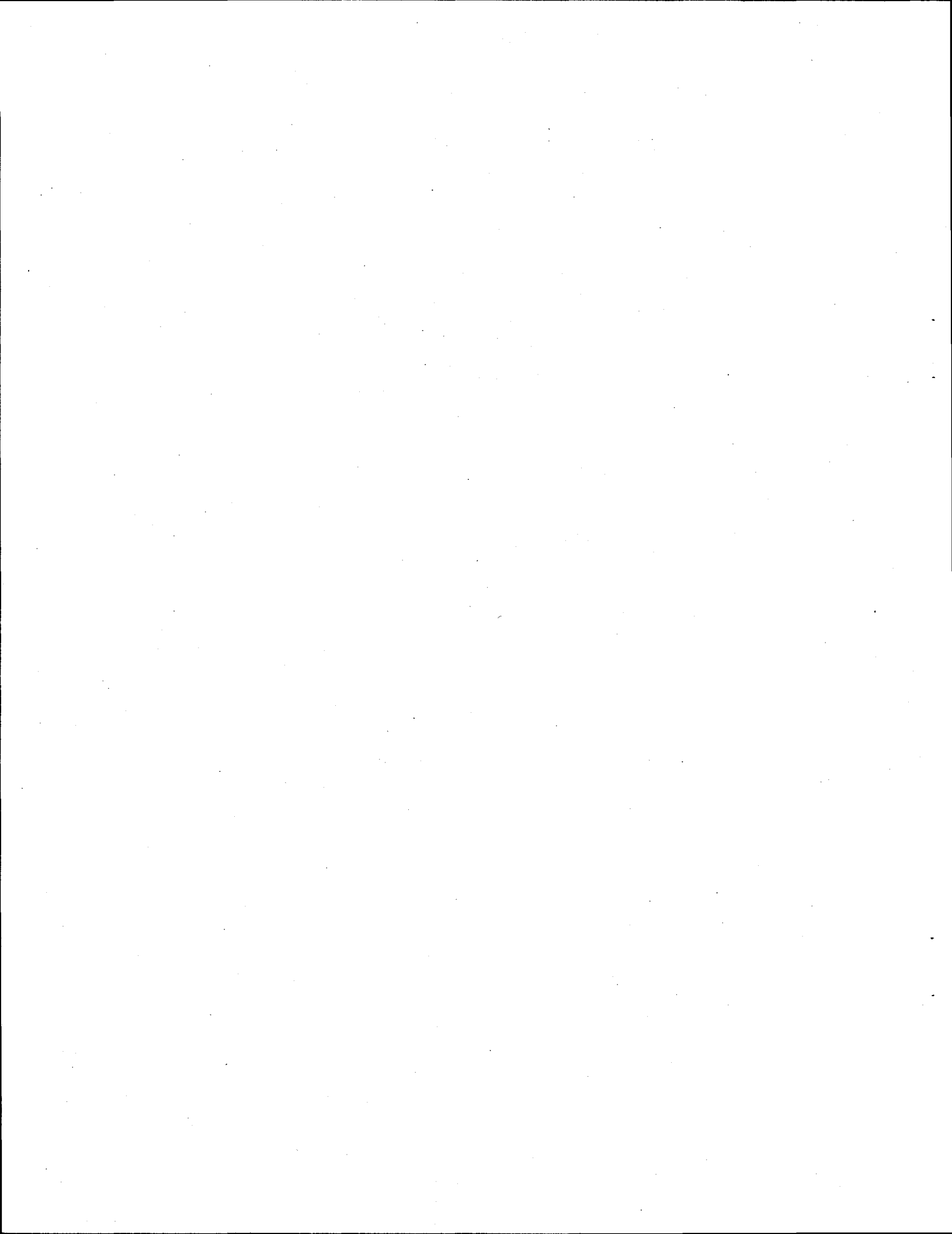
Acknowledgements

This work was supported by the Efficient Separations and Processing Crosscutting Program, Office of Science and Technology of the U.S. Department of Energy. We very much appreciate the encouragement and consistent support from Jim Buel, Joe Perez, Nick Lombardo, Bill Kuhn, Jud Virden, Bill Bonner, Rod Quinn, and John Sealock of Pacific Northwest National Laboratory for the development of SAMMS technology. We thank Wayne Cosby for his effective editorial help.



Glossary

PNNL	Pacific Northwest National Laboratory
SAMS	self-assembled monolayers
SAMMS	self-assembled mercaptan on mesoporous support
DOE	U.S. Department of Energy
RCRA	Resource Conservation and Recovery Act
UEFPC	Upper East Fork Poplar Creek
NPDES	National Pollution Discharge Emission Standard
SRL	Savannah River Laboratory
ICP-AES	inductively coupled plasma-atomic emission spectroscopy
TCLP	Toxicity Characteristic Leach Procedure
NRWTP	Non-Radiological Waste Water Treatment Plant
TEM	Transmission Electron Microscopy
XRD	x-ray diffraction
BET	Brunauer Emmett Teller (technology)
NMR	nuclear magnetic resonance
EXAFS	extended x-ray absorption fine structure
TMMPS	Tris-(methoxy)mercaptopropylsilane
CVAA	cold vapor atomic adsorption (spectroscopy)
ICP-MS	inductively coupled plasma-mass spectrometry
EDTA	ethylenediaminetetraacetic acid



Contents

Summary.....	iii
Acknowledgments.....	v
Glossary.....	vii
1.0 Introduction.....	1.1
2.0 Technology Needs for the Mixed Waste Focus Area.....	2.1
2.1 Alternative Technologies.....	2.1
3.0 Technology Description.....	3.1
3.1 The Scientific Principles.....	3.1
3.1.1 Self-Assembled Mercaptans on Oxide surfaces.....	3.1
3.1.2 Self-Assembled Mercaptans on Mesoporous Supports.....	3.1
3.2 Demonstrated Separation Performance.....	3.2
3.3 Generation of Secondary Wastes.....	3.3
3.4 The Cost Estimates for Technology Implementation.....	3.3
3.5 Materials Characterization.....	3.3
4.0 Mercury-Loading Capacity and Adsorption Kinetics of Thiol-SAMMS.....	4.1
4.1 Aqueous Speciation of Mercury.....	4.1
4.2 Kinetics Experiments.....	4.3
4.3 Adsorption Density Measurements.....	4.6
4.4 Free Energy of Adsorption.....	4.8
4.5 Distribution Coefficient Measurements.....	4.10
5.0 Effects of Organic Ligands on Mercury Adsorption by Thiol-SAMMS.....	5.1
6.0 Actinide Adsorption Characteristics of Functionalized SAMMS Material.....	6.1
7.0 Transition Metal Adsorption Characteristics of Thiol- SAMMS.....	7.1
8.0 Conclusions.....	8.1
8.1 Mercury-Adsorption Kinetics and Loading Capacity of Thiol-SAMMS.....	8.1
8.2 Effects of Organic ligands on Hg Adsorption by Thiol-SAMMS.....	8.1
8.3 Actinide Adsorption Characteristics of Functionalized SAMMS Material.....	8.1
8.4 Transition Metal Adsorption Characteristics of Thiol-SAMMS.....	8.2
9.0 References.....	9.1
Appendix A: Awards, Publications, and Press Highlights.....	A.1

Figures

Figure 4.1. Kinetics Data for Mercury Adsorption on Thiol-SAMMS as related to the Initial Mercury Concentrations and pH Values.....	4.5
Figure 4.2. Mercury Adsorption on Thiol-SAMMS as a Function of Uncomplexed Iodide Activity	4.9
Figure 6.1. Molecular Structures of 1,2-HOPO-SAMMS, 3,4-HOPO-SAMMS, and thiol-SAMMS	6.3

Tables

Table 4.1. Stability Constants and Solubility Product Constants used in Speciation Calculations.....	4.1
Table 4.2. Computed Speciation of Soluble Constituents (%) in the Equilibrating Solutions	4.3
Table 4.3. Kinetics Data for Hg Binding by thiol-SAMMS Material	4.4
Table 4.4. Matrix Solutions Used in Hg-Loading Experiments	4.6
Table 4.5. Mercury-Loading Data on SAMMS Obtained in Surrogate Solutions Containing Iodide Ions	4.7
Table 4.6. Comparison of Hg-Loading Data Obtained in Nitrate and Iodide Matrix Solutions	4.8
Table 4.7. Experimental Conditions Used for Measuring the Distribution Coefficients.....	4.10
Table 4.8. Distribution Coefficients for Adsorption of Hg by SAMMS Material from Surrogate Solutions.....	4.11
Table 5.1. Organic Ligand Effects on Hg Adsorption by thiol-SAMMS	5.22
Table 6.1. Actinide Absorption on Functionalized SAMMS.....	6.4
Table 7.1. Binding Affinity of Thiol-SAMMS for Selected Metal Species	7.1

1.0 Introduction

In 1992, scientists at Mobil Oil Research successfully synthesized ordered mesoporous materials using surfactant micellar structures as templates (Beck 1992; Kresge 1992). These materials have a very high surface area ($>1000 \text{ m}^2/\text{g}$), ordered pore structure (mostly hexagonal-packed cylindrical pore channels), and extremely narrow pore-size distribution. The pore diameter of these materials can be adjusted from 2 to 15 nanometers (nm). Mesoporous materials have been studied intensely since 1992 because of their great potential for applications in environmental and industrial processes. Numerous papers have been published on preparing novel chemical compositions from mesoporous materials and on studying the fundamentals of the reaction processes (Liu et al. 1996a and b). A wide range of mesoporous materials have been prepared, including alumina, zirconia, titania, niobia, tantalum oxide, and manganese oxide. Although the potential of mesoporous materials has been widely recognized, progress on the practical use of these novel materials has been slow. Many applications, such as adsorption, ion exchange, catalysis, and sensing, require the materials to have specific binding sites, stereochemical configuration or charge density, and acidity. Most mesoporous materials do not by themselves have appropriate surface properties; therefore, they need appropriate functionalization.

Pacific Northwest National Laboratory (PNNL)^(a) and other groups have developed a class of hybrid mesoporous materials, based on organized monolayers of functional molecules covalently bound to the mesoporous support (Liu et al. 1998; Feng et al. 1997a). The functional molecules are attached to the mesoporous support similarly to the preparation of self-assembled monolayers (SAMs) on flat substrates. This approach provides a unique opportunity to rationally engineer the surface properties. We have demonstrated that the hybrid mesoporous materials have exceptional selectivity and a capacity for adsorbing mercury (Hg) from contaminated waste streams. Recently, materials for removing other heavy metals, transition metals, radionuclides, etc, have also been demonstrated.

The purpose of this report is to summarize the results obtained in FY 98. The research during this fiscal year was aimed at 1) optimizing the performance of mesoporous materials under realistic operational conditions, 2) understanding the metal-loading kinetics and capacities, and 3) expanding the work to other metals, actinides, and organic species.

(a) Pacific Northwest National Laboratory is operated for the U.S. Department of Energy by Battelle under Contract DE-AC06-76RLO 1830.

2.0 Technology Needs for the Mixed Waste Focus Area

The U.S. Department of Energy (DOE) mixed-waste focus area has declared the removal and stabilization of Hg as the #1 and #4 priority need among 30 prioritized technology deficiencies (DOE 1996). Resource Conservation and Recovery Act (RCRA) metal and Hg removal has also been identified as a high-priority for site-specific needs by many DOE sites such as Albuquerque, Idaho Falls, Oak Ridge, Richland, Rocky Flats, and Savannah River (DOE 1991; DOE 1996).^(a) The proposed work will address DOE/EM's^(b) needs and these deficiencies. The development of self-assembled mercaptan on mesoporous support (SAMMS) technology provides opportunities for "breakthroughs" for RCRA metal and Hg removal/stabilization with significant cost and time reduction in the remediation process.

At the DOE Oak Ridge Site, an estimated 2.5-million pounds of Hg was lost to soil and surface water, and 3000 cubic feet of Hg is contained in plant sumps. The headwaters of Upper East Fork Poplar Creek (UEFPC), which are within the DOE Y-12 plant boundary, discharge 7-million gallons of water per day to Lower East Fork Poplar Creek. The UEFPC is contaminated with low levels of Hg. A Hg-reduction program at Oak Ridge Site has achieved point-source reduction, and Hg treatment systems are placed such that the Hg surface-water concentration is declining. However, these efforts have not been able to meet the National Pollution Discharge Emission Standard (NPDES) permit that requires that treatment to 0.012 mg/L is needed at UEFPC by April 27, 2000. Exceeding the anticipated limit triggers the requirement of monitoring methyl Hg in edible portions of fish present in contaminated streams (UEFPC). If the methyl-Hg concentration exceeds 1 mg/kg, the public must be protected from ingestion of fish.

Jim Klein of Westinghouse Savannah River Company has visited PNNL to discuss specific applications at Savannah River for removing Hg from the tritiated pump oil at the Savannah River Site.

2.1 Alternative Technologies

The existing technologies for RCRA metal and Hg removal from diluted wastewater include sulfur-impregnated carbon (Otani et al. 1988), microemulsion liquid membranes (Larson and Wiencek 1994), ion exchange (Ghazy 1995), and colloid precipitate flotation (Ritter and Bibler 1992). In the sulfur-impregnated carbon process, metal is adsorbed to the carbon, not covalently bound to the matrix as with SAMMS. The adsorbed metal needs secondary stabilization because the metal-laden carbon does not have the desired long-term chemical durability due to the weak bonding between the metal and the active carbon. In addition, a large portion of the pores in the active carbon is large enough for the entry of microbes to solubilize the Hg-sulfur compounds. The RCRA metal loading is not as high as that of mesoporous-based materials. The microemulsion liquid membrane technique uses an oleic acid microemulsion liquid membrane containing sulfuric acid as the internal phase to reduce the wastewater Hg concentration from 460 ppm to 0.84 ppm. However, it involves multiple steps of extraction,

(a) Klein, J. E., "R&D Needs for Mixed Waste Tritium Pump Oils (U)," Westinghouse Savannah River Company Inter-Office Memorandum, SRT-HTS-94-0235, July 11, 1994.

(b) EM = Environmental restoration and waste management.

stripping, de-emulsification, and recovery of Hg by electrolysis with use of large volumes of organic solvents. The liquid membrane swelling has a negative impact on extraction efficiency. The slow kinetics of the RCRA metal-ion exchanger reaction requires a long contacting time. This process also generates large volumes of organic secondary wastes. The ion exchange process uses Duolite™ GT-73 ion exchange organic resin to reduce the Hg level in wastewater from 2 mg/L to below 10 µg/L, but the oxidation of the resin results in substantially reduced resin life and an inability to reduce the Hg level to below the permitted level. The Hg loading is also limited. In addition, the Hg-laden organic resin does not have the ability to resist microbe attack. Hg can be released into the environment if it is disposed of as a waste form. The reported removal of RCRA metal from water by colloid precipitate flotation reduces the Hg concentration from 160 µg/L to about 1.6 µg/L. This process involves adding HCl to adjust the wastewater to pH 1, adding Na₂S and oleic acid solutions to the wastewater, and removing colloids from the wastewater. In this process, the treated wastewater is potentially contaminated with the Na₂S, oleic acid, and HCl by the treatment process. The separated Hg needs further treatment to be stabilized as a permanent waste form.

No existing technologies have been developed for removing Hg from pump oil. Some preliminary laboratory study of a zinc powder/filtration process was carried out by the Pantex Plant with certain success, but the work was discontinued due to losses of key personnel.

3.0 Technology Description

3.1 The Scientific Principles

This project focuses on a novel technology, SAMMS, for RCRA metal (i.e., Pb, Hg, Cd, Ag, etc.) removal/stabilization and Hg removal from organic solvents. The SAMMS materials are based on self-assembly of functionalized monolayers on mesoporous oxide surfaces.

3.1.1 Self-Assembled Mercaptans on Oxide surfaces

The self-assembled mercaptan provides three important functions: 1) molecular recognition for metals, 2) covalent bonding to the support materials, and 3) a high population density of the functional groups on the substrate surfaces.

Molecular self-assembly is a unique phenomenon in which functional molecules aggregate on an active surface, resulting in an organized assembly having both order and orientation (Bunker et al. 1993; Whitesides 1996; Bishop and Nuzzo 1996). In this approach, bifunctional molecules containing a hydrophilic head group and a hydrophobic tail group adsorb onto a substrate or an interface as closely-packed monolayers. The driving forces for the self-assembly are the intermolecular interactions (such as van der Waals forces) between the functional molecules. The tail group and the head group can be chemically modified to contain certain functional groups to promote covalent bonding between the functional organic molecules and the substrate on one end, and the molecular bonding between the organic molecules and the metals on the other. By populating the outer interface with alkylthiols (which are well known to have a high affinity for various heavy metals, including Hg), an effective means for scavenging heavy metals is made available. For functionalizing mercaptan-related compounds can be used, which are effective antidotes for treating patients with Hg poisoning (Mitra 1986). A high surface area of such functionalized support allows for high loading of RCRA metals.

3.1.2 Self-Assembled Mercaptans on Mesoporous Supports

The unique mesoporous oxide supports provide a high surface area ($>1000 \text{ m}^2/\text{g}$), thereby enhancing the metal-loading capacity. They also provide an extremely narrow pore size distribution, which can be specifically tailored from 15 \AA to 400 \AA , thereby minimizing biodegradation from microbes and bacteria. Because of their non biodegradability, used mesoporous structures can be disposed of as stable waste forms.

The porous supporting materials used for this purpose (SiO_2 , ZrO_2 , TiO_2) are synthesized through a co-assembly process using oxide precursors and surfactant molecules. The materials are synthesized by mixing surfactants and oxide precursors in a solvent and exposing the solution to mild hydrothermal conditions. The surfactant molecules form ordered liquid crystalline structures, such as hexagonally ordered rod-like micelles, and the oxide materials precipitate on the micellar surfaces to replicate the organic templates formed by the rod-like micelles. Subsequent calcination to 500°C removes the surfactant templates and leaves a high surface-area oxide skeleton. The pore size of the mesoporous materials is then determined by the rod-like

micelles, which are extremely uniform. Using surfactants of different chain length produces mesoporous materials with different pore sizes.

3.2 Demonstrated Separation Performance

The most important separation performance of SAMMS can be summarized as

- **High RCRA Metal Loading:** The high surface area of the mesoporous oxides ($>1000 \text{ m}^2/\text{g}$) ensures a large capacity for metal loading (up to 0.7 g Hg per gram of SAMMS)
- **High Selectivity:** Self-assembled functional groups, such as mercaptans, provide a high affinity and selectivity for RCRA metals, such as Hg, Ag, Pb, Cd, and Co, without interference from other abundant cations (such as alkaline and alkaline earths) in wastewater and in soils.
- **High Flexibility:** The binding of different forms of Hg, including metallic, inorganic, organic, charged, and neutral compounds, removes the Hg from both aqueous wastes and organic wastes, such as vacuum pump oils; this process can clean up wastewater as well as gaseous wastes, sludge, sediment, and soil.
- **Stable Waste Form:** The Hg-loaded SAMMS not only pass Toxicity Characteristic Leach Procedure (TCLP) tests, but also have good long-term durability as a waste form because 1) the covalent binding between Hg and SAMMS has good resistance in ion-exchange, oxidation, and hydrolysis over a wide pH range and 2) the uniform and small pore size (2 to 40 nm) of the mesoporous silica prevents bacteria (at least 2000 nm in size) from solubilizing the bound Hg (microbes are mainly responsible for solubilizing the Hg compounds in the environment into the deadly methyl Hg). The SAMMS technology is superior to many existing technologies because of the direct generation of a stable waste form that does not require secondary treatment.
- The SAMMS materials can be also fabricated into various engineering forms such as pellets, columns, or films. They have good mechanical strengths and are very durable and stable in air and in aqueous solution.

Procedures for self-assembly of a variety of functional molecules on oxide surfaces have been extensively investigated and developed at PNNL. Procedures for synthesizing mesoporous silica, zirconia, alumina, and titania supports have been developed at PNNL and by other groups as well. The procedure for making SAMMS is currently being optimized. Several types of SAMMS materials have been recently synthesized. Surface characteristics of the mesoporous support plays a significant role in anchoring the mercaptans on the surface. Boiling mesoporous silica in water increases the number of silanols on the surface, thereby providing the foundation for the self-assembly of the mercaptan.

Preliminary trials of the Hg-binding abilities of SAMMS were conducted in simulated wastewater of Savannah River Laboratory (SRL) radioactive-waste holding Tank L and simulated nonradioactive vacuum pump oil waste of the SRS tritium facilities. These waste

solutions were mixed with SAMMS powders at volume ratios of waste to SAMMS ranging from 20 to 100 at room temperature for 2 hours. The remaining RCRA metals in solutions were analyzed using cold-vapor atomic absorption for Hg and inductively coupled plasma-atomic emission spectroscopy (ICP-AES) for other metals. SAMMS reduced the Hg concentration from 6.35 ppm to 0.7 ppb (below the drinking water limit of 2 ppb) by just one treatment of wastewater 38 times its volume. The distribution coefficient is as large as 340,000 at a pH range from 3 to 9 and with the presence of large concentrations of other cations (e.g., 2220 ppm Na). The RCRA metals, Pb, Ag, and Cr, were also reduced to below RCRA levels at pH 7 and 9. SAMMS reduced the Hg level from 12.1 mg/L to 0.066 mg/L (the hazardous waste limit is 0.2 mg/L) by treating 20 times the waste-oil volume once. The RCRA-laden SAMMS can be disposed of directly as solid wastes since they passed Toxicity Characteristic Leach Procedure (TCLP) tests by showing up to 1000 times lower release of RCRA metals.

3.3 Generation of Secondary Wastes

No secondary wastes will be generated during the application of SAMMS for clean up since no chemicals, washing solution, regeneration, and secondary treatment are involved. The RCRA metal-laden SAMMS can be directly disposed of as nonhazardous solid wastes.

3.4 The Cost Estimates for Technology Implementation

A preliminary cost estimate of applying the SAMMS materials for the removal of Hg from waste water treated at the Non-Radiological Wastewater Treatment Plant (NRWTP) at the Oak Ridge National Laboratory was completed. A comprehensive model has been established and is being tested. This model is capable of evaluating the effects of Hg concentration, the waste volume, flow rate, column size, capital cost, frequency of regeneration or replacement, waste disposal, etc., on the total operational cost for any particular waste stream.

The assessment for Oak Ridge indicates that SAMMS offers a method for improved Hg removal that may be significantly less expensive than other options. The cost estimate of manufacturing SAMMS was \$21.60/kg of SAMMS with a market price estimated to be approximately \$50/kg or 1400/ft³. This cost estimate may be compared to other separations materials that range from \$29/kg for zeolite beta to \$100/kg for crystalline-silicotitanates (a cesium ion exchange material) to thousands of dollars per kg for high-grade chromatography materials produced in relatively low quantities. A comparison of the cost of the materials and waste disposal reflects the high capacity and selectivity of the SAMMS. The cost per kg of Hg removed was estimated to be \$710 for the SAMMS, \$6960 for GT-73 (a commercially available, organic-based sorbent) and \$261,000 for activated carbons. The high Hg loading on the SAMMS results in a small volume of material, minimizing the cost of material procurement and waste disposal.

3.5 Materials Characterization

The pore structure and chemical composition of the hybrid mesoporous materials can be studied by transmission electron microscopy (TEM), low angle X-ray diffraction (XRD), and the Brunauer-Emmett-Teller (BET) techniques. TEM studies suggest that the hexagonal structures

remain the same after attaching the functional molecules and after absorbing metal ions. BET shows that the monolayers inside the pore channels have reduced the pore diameter by about 8 Å. In addition, the structure of the functional monolayers and the chemical bonding can be studied by solid-state nuclear magnetic resonance (NMR) and extended x-ray absorption fine structure (EXAFS) techniques. Multinuclear solid state NMR measurements provide direct information on the local environment of nuclear active elements (such as ^{13}C and ^{29}Si) through chemical shifts, coupling between different nuclear spins, and electrical-field gradient. EXAFS probes the distribution of neighboring atoms at a particular atomic position (Hg).

Based on the TEM, NMR, and EXAFS experiments, the molecular conformation of the monolayers has been established. At low surface coverage, the carbon chains can adapt a wide range of conformations, as indicated by a single broad ^{13}C NMR resonance formed from the two carbon atoms next to the thiol group. Under this condition, the siloxane groups can adopt three different conformations: 1) isolated groups that are not bound to any neighboring siloxanes, 2) terminal groups that are only bound to one neighboring siloxane, and 3) cross-linked groups that are bound to two neighboring siloxanes. Among the three groups, the terminal conformation (2) is dominant. At higher population densities, all of the carbon chains are near one another, closely packed, and have a vertical orientation with respect to the silica surface. The NMR resonance peaks from all three carbon atoms in the backbone are well-resolved. NMR spectra for ^{29}Si show the predominance of only cross-linked bonding conformation for the siloxanes rather than a distribution of isolated, terminal, and cross-linked groups. When heavy metal (Hg) binds to the thiol group, the peak position and shape of the terminal head group in ^{13}C spectra are also affected. From the EXAFS data, Hg-S and Hg-O bond lengths are calculated as $2.4 \pm 0.01 \text{ \AA}$ and $2.14 \pm 0.01 \text{ \AA}$, respectively. The Hg atoms on the two adjacent thiol groups are linked by the same oxygen atom with a Hg-Hg separation of $3.99 \pm 0.05 \text{ \AA}$, and the bond angle of Hg-O-Hg is calculated as 137° . The functional molecules are estimated to be about 4 Å apart, with each molecule occupying 16 \AA^2 on the surface. This number is consistent with the lateral dimension of the TMMPS molecules.

4.0 Mercury-Loading Capacity and Adsorption Kinetics of Thiol-SAMMS

One of the technologies being tested involves mobilizing Hg from solid wastes using a lixiviant consisting of an aqueous solution of KI/I₂ (Foust 1993). This patented process uses solutions consisting of I₂ (0.001 to 0.5 M) as the oxidizing agent and the iodide ion (from 0.1 to 1.0 M) as a complexing ligand. Hg in contaminated solid wastes in the form of oxides, sulfides, elements, solid-solution phases and as adsorbed phase is mobilized by the KI/I₂ lixiviant through oxidation and complex formation reactions. After such mobilization, the dissolved, strongly complexed Hg needs to be removed before the lixiviant is recycled.

The objective of this study is to demonstrate the effectiveness of the thiol-SAMMS for removing Hg from spent potassium iodide/iodine (KI/I₂) lixiviant. This study included an investigation of aqueous speciation, kinetics, loading capacity, and the distribution coefficient for Hg adsorption on SAMMS material. The parameters studied included varying ionic strengths and iodide concentrations, pH conditions, and soluble Hg concentrations.

4.1 Aqueous Speciation of Mercury

The adsorption of Hg is influenced by the types and concentrations of aqueous species of Hg and other competing cations that are present in the waste solutions. To help interpret the adsorption data, the aqueous speciation of Hg in different matrix solutions was calculated using an equilibrium code, GEOCHEM (Mattigod and Sposito 1979; Mattigod 1996; Mattigod and Zachara 1997a). The association constants for aqueous complexes and the solubility product constants of solid phases used in the computations are listed in Table 4.1.

Table 4.1. Stability Constants and Solubility Product Constants used in Speciation Calculations

Reaction	log K	Source
Aqueous Species		
$\text{Hg}^{2+} + \text{NO}_3^- = \text{HgNO}_3^+$	0.77	1
$\text{Hg}^{2+} + 2\text{NO}_3^- = \text{Hg}(\text{NO}_3)_2^0$	1.00	1
$\text{Hg}^{2+} + \text{OH}^- + \text{NO}_3^- = \text{HgOHNO}_3^0$	11.70	4
$\text{Hg}^{2+} + \text{OH}^- = \text{HgOH}^+$	10.60	1
$\text{Hg}^{2+} + 2\text{OH}^- = \text{Hg}(\text{OH})_2^0$	21.80	1
$\text{Hg}^{2+} + 3\text{OH}^- = \text{Hg}(\text{OH})_3^-$	20.90	1
$2\text{Hg}^{2+} + \text{OH}^- = \text{Hg}_2\text{OH}^{3+}$	10.70	1
$3\text{Hg}^{2+} + 3\text{OH}^- = \text{Hg}_3(\text{OH})_3^{3+}$	35.60	1
$\text{Hg}^{2+} + \text{I}^- = \text{HgI}^+$	13.41	1
$\text{Hg}^{2+} + 2\text{I}^- = \text{HgI}_2^0$	24.68	1
$\text{Hg}^{2+} + 3\text{I}^- = \text{HgI}_3^-$	28.41	1
$\text{Hg}^{2+} + 4\text{I}^- = \text{HgI}_4^{2-}$	30.30	1

Reaction	log K	Source
$\text{Hg}^{2+} + \text{OH}^- + \text{I}^- = \text{HgOH}^0$	23.46	1
$\text{Hg}^{2+} + \text{SO}_4^{2-} = \text{HgSO}_4^0$	2.50	1
$\text{Hg}^{2+} + 2\text{SO}_4^{2-} = \text{Hg}(\text{SO}_4)_2^{2-}$	3.48	1
$\text{Hg}^{2+} + \text{HSO}_4^- = \text{HgHSO}_4^+$	1.10	5
$\text{Hg}^{2+} + \text{OH}^- + \text{SO}_4^{2-} = \text{HgOHSO}_4^-$	12.94	4
$\text{Ca}^{2+} + \text{NO}_3^- = \text{CaNO}_3^+$	0.50	3
$\text{Ca}^{2+} + 2\text{NO}_3^- = \text{Ca}(\text{NO}_3)_2^0$	0.60	1
$\text{Ca}^{2+} + \text{I}^- = \text{CaI}^+$	0.07	5
$\text{Ca}^{2+} + \text{OH}^- = \text{CaOH}^+$	1.30	1
$\text{Ca}^{2+} + 2\text{OH}^- = \text{Ca}(\text{OH})_2^0$	0.00	7
$\text{Ca}^{2+} + \text{SO}_4^{2-} = \text{CaSO}_4^0$	2.30	3
$\text{Fe}^{2+} + \text{OH}^- = \text{FeOH}^+$	4.70	2
$\text{Fe}^{2+} + 2\text{OH}^- = \text{Fe}(\text{OH})_2^0$	7.40	2
$\text{Fe}^{2+} + 3\text{OH}^- = \text{Fe}(\text{OH})_3^-$	9.30	2
$\text{Fe}^{2+} + 4\text{OH}^- = \text{Fe}(\text{OH})_4^{2-}$	8.90	2
$\text{Fe}^{2+} + \text{SO}_4^{2-} = \text{FeSO}_4^0$	2.20	1
$\text{Fe}^{2+} + 2\text{SO}_4^{2-} = \text{Fe}(\text{SO}_4)_2^{2-}$	0.76	1
$\text{Fe}^{2+} + \text{HSO}_4^- = \text{FeHSO}_4^+$	1.08	8
$\text{Fe}^{2+} + \text{NO}_3^- = \text{FeNO}_3^+$	0.30	8
$\text{Fe}^{2+} + \text{I}^- = \text{FeI}^+$	3.67	5
$\text{Fe}^{2+} + 2\text{I}^- = \text{FeI}_2^0$	5.80	5
$\text{Fe}^{2+} + \text{OH}^- + \text{I}^- = \text{FeOH}^0$	6.90	4
$\text{K}^+ + \text{NO}_3^- = \text{KNO}_3^0$	-0.19	3
$\text{K}^+ + \text{I}^- = \text{KI}^0$	-0.19	1
$\text{K}^+ + \text{SO}_4^{2-} = \text{KSO}_4^-$	0.85	3
$\text{K}^+ + \text{OH}^- = \text{KOH}^0$	-0.50	1
$\text{H}^+ + \text{SO}_4^{2-} = \text{HSO}_4^-$	1.99	1
$\text{H}^+ + \text{OH}^- = \text{H}_2\text{O}$	14.00	1

Reaction	log K_{sp}	Source
----------	--------------	--------

Solid Phases

$\text{Hg}^{2+} + 2\text{OH}^- = \text{H}_2\text{O} + \text{HgO}(\text{s})$	25.44	1
$\text{Hg}^{2+} + \text{SO}_4^{2-} = \text{HgSO}_4(\text{s})$	3.30	6
$\text{Ca}^{2+} + 2\text{OH}^- = \text{Ca}(\text{OH})_2(\text{s})$	5.19	1
$\text{Ca}^{2+} + \text{SO}_4^{2-} + 2\text{H}_2\text{O} = \text{CaSO}_4 \cdot 2\text{H}_2\text{O}(\text{s})$	4.62	2
$\text{Fe}^{2+} + 2\text{OH}^- = \text{Fe}(\text{OH})_2(\text{s})$	14.40	1

¹Smith and Martell (1976). ²Martell and Smith (1982). ³Smith and Martell (1989). ⁴Dyrssen et al. 1968, ⁵Estimated Nieber and McBryde 1973. ⁶Calculated from ΔG data from Wagman et al. 1969. ⁷Greenberg and Copeland (1960).

⁸Mattigod and Sposito 1977.

The speciation calculations showed that about 92 to 99% of the total dissolved Hg in equilibrating solutions existed as HgI_4^{2-} species (Table 4.2). The remaining fraction of the dissolved Hg was predicted to be in the form of HgI_3^- species (1 to 8%). In these solutions, no solid precipitation reactions were predicted to occur; thus Hg in these systems would occur only in dissolved and adsorbed forms. Further, the Hg speciation indicates that adsorption reactions would be controlled by the concentration (activity) of the dominant form namely, HgI_4^{2-} species. The speciation of other dissolved constituents such as K, Ca, and Fe are also listed in Table 4.2.

Table 4.2. Computed Speciation of Soluble Constituents (%) in the Equilibrating Solutions

<u>Species</u>	<u>Equilibrating Solution</u>				
	<u>S1</u>	<u>S2</u>	<u>S3</u>	<u>S4</u>	<u>S5</u>
HgI_4^{2-}	98.9	98.2	97.7	97.1	92.3
HgI_3^-	1.1	1.2	2.3	2.9	7.7
K^+	87.0	88.0	86.6	88.0	87.2
KI^0	11.6	9.7	8.2	6.2	2.3
KSO_4^-	1.4	2.3	5.2	5.8	10.5
Ca^{2+}	81.8	76.5	65.0	63.4	50.8
CaI^+	10.9	8.8	6.6	4.6	1.4
CaSO_4^0	7.3	14.7	28.4	32.0	47.8
FeI_2^0	96.5	95.9	95.3	93.8	84.5
FeI^+	3.5	4.1	4.7	6.2	15.3

4.2 Kinetics Experiments

A set of experiments was designed to study the kinetics of adsorption of dissolved Hg from a matrix solution of 100 mmol/L KI. The binding kinetics were assessed using batch adsorption experiments at four different pH values, ranging from acidic to basic (3, 5, 7, and 9). The rates of adsorption were monitored by measuring the Hg concentration in the solution phase at selected periodic intervals. Because the rate of adsorption is affected by the initial concentration of adsorbate, two sets of kinetic experiments at each pH value were conducted to examine this phenomenon. The initial Hg concentrations in these experiments were set at ~0.5 and ~1.8 mmol/L, respectively. These concentrations were selected on the basis that this range of Hg concentration may represent the higher range found in KI solution following extraction of actual Hg-bearing wastes. A fixed solid:solution ratio of 1:800 was used in all experiments. The test matrix for the adsorption kinetic studies consisted of eight experiments with seven periodic measurements (5, 10, 30, 60, 120, 180, and 360 mins) of Hg concentration in each experiment.

The results of the binding kinetics experiments are listed in Table 4.3. The speciation calculations indicated that all dissolved Hg existed as anionic iodide complexes (~92% as HgI_4^{2-}

and ~8% as HgI_3^-). The data show that at initial Hg concentrations of 0.5 mmol/L and at all pH values, ~95% of the final adsorption occurs within the first 5 min (Table 4.3, Figure 4.1). No significant differences in the rate of adsorption (rate of decrease in solution concentration) were observed at pH values of 5, 7, and 9; however, at pH 3, the rate appeared to be lower than that observed at higher pH values. In all cases, adsorption equilibrium seems to have been attained in ~4 h.

In experiments with higher initial concentrations of Hg (1.8 mmol/L), the rates of adsorption at all pH values were slightly slower than that observed at lower initial Hg concentrations (0.8 mmol/L). On average, ~82% final adsorption occurred within the first 5 min (Table 4.3, Figure 4.1). No significant differences in the rate of adsorption (rate of decrease in solution concentration) were observed at pH values of 3, 5, and 7; however, at pH 9, the rate appeared to be slightly higher than observed at lower pH values. Also in this set of experiments, adsorption equilibrium seems to have been attained in ~4 h. The rapid rates of Hg adsorption onto SAMMS materials observed in these experiments are similar to the reaction rates observed previously by Feng et al. (1997b) for adsorption on SAMMS in 0.1 M NaNO_3 solutions with very low initial concentrations of Hg (0.5 and 10 mg/L). In an NaNO_3 medium, the speciation calculations show that the dissolved Hg exists mainly in the form of neutral hydrolytic species $[\text{Hg}(\text{OH})_2^0]$. Therefore, these tests show that the dissolved Hg is adsorbed with extreme rapidity irrespective of the type and charge of Hg complex species $[\text{HgI}_4^{2-}$ or $\text{Hg}(\text{OH})_2^0]$ in waste solution.

Table 4.3. Kinetics Data for Hg Binding by thiol-SAMMS Material

pH	Time (min)	Conc. (mg/L)	Adsorbed (mg/g)	pH	Time (min)	Conc. (mg/L)	Adsorbed (mg/g)
3	0	102.0	0.0	3	0	375.0	0.0
3	5	14.2	70.2	3	5	184.0	152.8
3	10	11.9	72.1	3	10	163.5	169.2
3	30	11.0	72.8	3	30	159.0	172.8
3	60	10.1	73.5	3	60	139.0	188.8
3	120	8.3	75.0	3	120	150.0	180.0
3	180	8.3	75.0	3	180	141.0	187.2
3	360	7.8	75.4	3	360	141.0	187.2
5	0	102.0	0.0	5	0	358.0	0.0
5	5	6.1	76.8	5	5	170.5	150.0
5	10	4.2	78.2	5	10	156.0	161.6
5	30	3.7	78.7	5	30	140.0	174.4
5	60	3.0	79.2	5	60	124.0	187.2
5	120	2.7	79.4	5	120	135.0	178.4
5	180	2.6	79.6	5	180	126.0	185.6
5	360	2.1	80.0	5	360	123.0	188.0

7	0	101.0	0.0	7	0	358.0	0.0
7	5	7.0	75.2	7	5	170.5	150.0
7	10	5.2	76.7	7	10	153.5	163.6
7	30	4.5	77.2	7	30	145.0	170.4
7	60	3.5	78.0	7	60	134.0	179.2
7	120	3.5	78.0	7	120	134.0	179.2
7	180	2.95	78.5	7	180	130.0	182.4
7	360	2.6	78.7	7	360	127.0	184.8
9	0	99.5	0.0	9	0	382.0	0.0
9	5	5.9	74.9	9	5	160.0	177.6
9	10	4.5	76.0	9	10	147.0	188.0
9	30	3.7	76.7	9	30	144.0	190.4
9	60	2.8	77.4	9	60	150.0	185.6
9	120	2.6	77.5	9	120	130.0	201.6
9	180	2.6	77.5	9	180	122.0	208.0
9	360	2.0	78.0	9	360	122.0	208.0

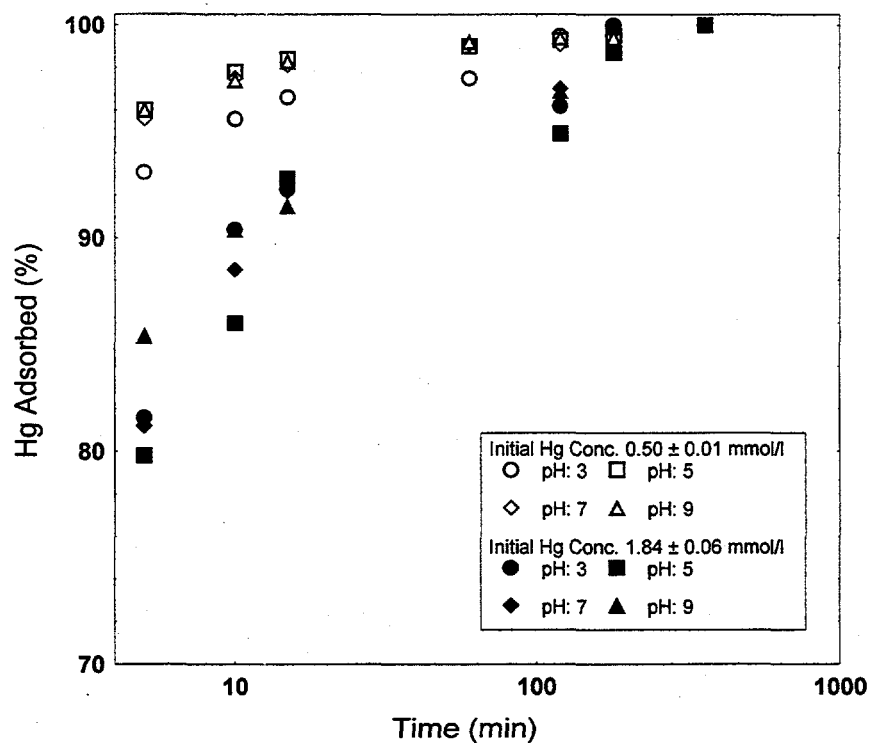


Figure 4.1. Kinetics Data for Mercury Adsorption on Thiol-SAMMS as related to the Initial Mercury Concentrations and pH Values

4.3 Adsorption Density Measurements

The objective of these experiments was to measure the range of Hg loading on thiol-SAMMS material that can be achieved from matrix solutions formulated as surrogates for leachates from actual Hg-containing wastes. The compositions of surrogate solutions were developed on the basis of the composition of actual leachates resulting from spent KI lixiviant. According to the actual leachate data, the dominant dissolved constituents in the actual Hg-containing waste streams are K^+ , I^- , and I_2 , with minor amounts of Fe^{2+} and SO_4^{2-} . Based on this information, a series of surrogate solutions was prepared, containing varying concentrations of I, K, Hg, and other minor constituents. These solutions were formulated to represent varying compositions of leachates, washwaters, and combinations of these waste streams. The Hg concentrations used in these experiments ranged from ~0.5 to 2.9 mmol/L.

Generally, the contaminant loading on an exchange material is affected by several factors, such as the composition of the matrix solution (competing ions, ionic strength, and pH), concentration of contaminant, solid:solution ratio, and contact time. In this set of experiments, the effects of KI concentrations and solid:solution ratios were tested with a fixed contact time of 4 h. The compositions of the surrogate test solutions used in these experiments are listed in Table 4.4. The loading experiments were conducted in duplicate (except two very high solid:solution ratio experiments), with surrogate solutions and varying quantities of SAMMS material to achieve ratios ranging from 1:200 to 1:4000. The surrogate solutions were contacted with SAMMS material for 4 h to achieve equilibrium. Following equilibrium, the solutions were separated from the SAMMS material using 0.2- μ m syringe filters. The Hg concentrations in the equilibrated solutions were determined by cold vapor atomic adsorption spectroscopy (CVAA) and analyzed for residual Hg concentrations and pH.

Table 4.4. Matrix Solutions Used in Hg-Loading Experiments

Constituent (mmol/L)	Solutions				
	S1	S2	S3	S4	S5
Iodide	606	410	350	250	90
Sulfate	20	23	54	54	88
K	635	440	450	350	265
Fe (II)	3	3	2	2	0.5
Ca	--	--	0.1	0.1	0.2
Hg	2.34	2.89	1.30	1.69	0.49

The data show that SAMMS loading can range from 26 to 270 mg/g, depending on the composition of the matrix solution and the solid:solution ratio (Table 4.5). The results indicate that at a fixed solid:solution ratio with sufficient Hg to saturate the adsorption sites, the loading density increases with decreasing iodide concentrations. At both solid:solution ratios (1:200 and 1:800), ~40% reduction in iodide concentrations resulted in ~50% increase in Hg loading by

SAMMS. Such increase in loading with decreasing iodide concentrations suggests that iodide influences Hg adsorption through complex formation. A five-fold change in solid:solution ratio (1:800 to 1:4000) at a fixed iodide and initial Hg concentration resulted in an ~50% increase in Hg loading on SAMMS, indicating that increasing solid:solution ratios also increase Hg loading. The highest Hg loading of 270 mg/g of SAMMS was observed when K concentration in the matrix solution was 265 mmol/L at a solid:solution ratio of 1:4000.

These Hg-loading data may be compared to previous loading data (Feng et al., 1997b) on SAMMS (solid:solution ratio 1:5000) obtained in matrix solutions consisting of 100 mmol/L NaNO₃ with initial Hg concentrations ranging from 0.00024 to 670 mg/L. Loading densities of 83 to 635 mg/g observed in previous experiments indicate that NaNO₃ media do not influence Hg loading on SAMMS to the same extent that the KI-K₂SO₄ media do in these experiments. Data obtained in previous and current studies under somewhat similar experimental conditions (solid:solution ratio and initial Hg concentration) show that in a KI-K₂SO₄ medium, the loading achieved is about one-half of the loading density attained in a NaNO₃ matrix solution (Table 4.6). Calculated speciation indicates that in NaNO₃ media, dissolved Hg exists in the form of Hg²⁺ (37%), Hg(OH)₂⁰ (30%), HgOH⁺ (14%), HgOHNO₃⁰ (10%), and HgNO₃⁺ (9%). In comparison, in a KI-K₂SO₄ medium, dissolved Hg exists as HgI₄²⁻ (92%) and HgI₃⁻ (8%). These data comparisons suggest that anionic Hg-I complexes are adsorbed to a lesser extent by SAMMS as compared to the free and cationic and neutral complexes of Hg. These data clearly indicate that Hg speciation in solution significantly influences the extent of adsorption on SAMMS material.

Table 4.5. Mercury-Loading Data on SAMMS Obtained in Surrogate Solutions Containing Iodide Ions

<u>Solution</u>	<u>Replicate</u>	<u>Solid: Solution Ratio</u>	<u>I Conc. (mmol/L)</u>	<u>Equil. Hg Conc. (mmol/L)</u>	<u>Hg Loading (mg/g)</u>
S1	1	1:200	606	1.695	26
S1	2	1:200	606	1.645	28
S2	1	1:800	410	2.393	78
S2	2	1:800	410	2.443	70
S3	1	1:200	350	0.273	41
S3	2	1:200	350	0.276	41
S4	1	1:800	250	1.047	105
S4	2	1:800	250	0.997	113
S4	1	1:4000	250	1.496	165
S5	1	1:800	90	0.003	77
S5	2	1:800	90	0.002	84
S5	1	1:4000	90	0.150	270

Table 4.6. Comparison of Hg-Loading Data Obtained in Nitrate and Iodide Matrix Solutions

<u>Matrix Solution</u>	<u>Initial Hg Conc. (mmol/L)</u>	<u>Solid:Solution Ratio</u>	<u>Hg- Loading (mg/g) of SAMMS</u>	<u>Source</u>
KI	0.489	1:4000	270	This Study
NaNO ₃	0.563	1:5000	415	Feng et al. 1997b

4.4 Free Energy of Adsorption

The speciation calculations showed that HgI_4^{2-} species was the dominant form (92 to 99%) of the total dissolved Hg. Therefore, adsorption of dissolved Hg on SAMMS material can occur through dissociation of HgI_4^{2-} in to free ionic Hg and subsequent adsorption on to thiol groups as follows:



The overall reaction as the sum of reactions (1) and (2) can be represented as



The equilibrium constants as a function of activities of reactants and products in the above reactions are expressed as

$$K_1 = (\text{Hg}^{2+})(\text{I}^-)^4 / (\text{HgI}_4^{2-}) \quad (4.4)$$

$$K_2 = (-\text{RS}_2\text{Hg})(\text{H}^+)^2 / (-\text{RSH})^2(\text{Hg}^{2+}) \quad (4.5)$$

$$K_3 = (-\text{RS}_2\text{Hg})(\text{H}^+)^2(\text{I}^-)^4 / (-\text{RSH})^2(\text{HgI}_4^{2-}) \quad (4.6)$$

The equilibrium constant K_3 can be evaluated using the computed activities of HgI_4^{2-} and free ionic I species, the measured pH, and calculated adsorbed phase activity of Hg (calculated as equivalent to mole fraction adsorbed). Equation (4.6) can be solved graphically using a linearized form as:

$$\log K_3 = \log(N_{\text{Hg}}) - 2\text{pH} + 4\log(\text{I}^-) - 2\log(N_{\text{H}}) + \log(\text{HgI}_4^{2-}) \quad (4.7)$$

Rearranging equation (4.7) results in

$$Y = -4\log(\text{I}^-) + \log K_3 \quad (4.8)$$

where $Y = \log(N_{\text{Hg}}) - 2\text{pH} - 2\log(N_{\text{H}}) + \log(\text{HgI}_4^{2-})$.

A plot of Y as the dependent and $\log(I^-)$ as the independent variable would yield a slope of -4 and an intercept equal to $\log K_3$. Plotting adsorption data yielded a line with a slope of -3.8 and an intercept of -11.45 (Figure 4.2). Using the value of $\log K_3$ (-11.45) and the value of $\log K_1$ (-30.3 from Table 4.1), the value $\log K_2$ was calculated as

$$\log K_2 = \log K_2 - \log K_1 = -11.45 - (-30.3) = 18.85 \quad (4.9)$$

From this $\log K_2$ value, the free energy of exchange for the reaction



was calculated to be -107.6 kJ/mol of Hg^{2+} . This value indicates a significantly higher affinity by Hg^{2+} for the thiol groups as compared to other divalent metal affinity for silanol groups (an average free energy of exchange value of about -60 kJ/mol). The higher affinity of Hg^{2+} for thiol groups can be explained on the basis of soft-cation/soft-base interaction in which the soft cation can very easily displace protons.

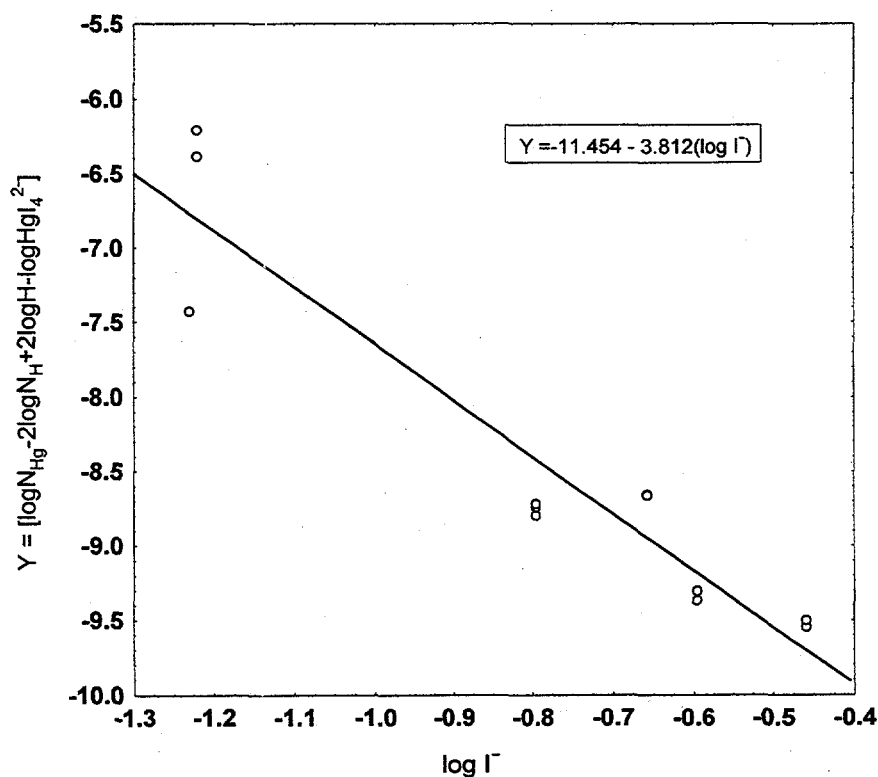


Figure 4.2. Mercury Adsorption on Thiol-SAMMS as a Function of Uncomplexed Iodide Activity

4.5 Distribution Coefficient Measurements

The distribution coefficient is an empirical measure of an exchange substrate's selectivity or specificity for adsorbing a specific contaminant or a group of contaminants from matrix solutions, such as waste streams. The distribution coefficient (sometimes referred to as the partition coefficient at equilibrium) is defined as a ratio of the adsorption density to the final contaminant concentration in solution at equilibrium. This measure of selectivity is defined as

$$K_d = A_{eq} / C_{eq} \quad (4.11)$$

where K_d is the distribution coefficient (mL/g), A_{eq} is the equilibrium adsorption density (mg of contaminant per gram of adsorbing substrate), and C_{eq} is the contaminant concentration (mg/mL) in contacting solution at equilibrium. The partition coefficient is defined as

$$K_p = A/C \quad (4.12)$$

where K_p is the partition coefficient (mL/g), A is the adsorption density (mg of contaminant per gram of adsorbing substrate) at any stage before equilibrium is attained, and C is the contaminant concentration (mg/mL) in contacting solution at the same stage as the adsorption is calculated. At equilibrium, the K_p will be equal to K_d .

The K_d s were measured by equilibrating 25- and 100-mg quantities of SAMMS material with 20 mL of contact solution (solid:solution ratios of 1:800 and 1:200, respectively). The contact solutions were formulated with two different Hg concentrations (~0.3 and ~0.5 mmol/L). The concentrations of major constituents in both solutions consisted of ~270 mmol of potassium, ~90 mmol/L of iodide, ~90 mmol/L of sulfate, and minor concentrations of Fe (II) and calcium. The solution compositions used in these experiments are listed in Table 4.7. Following 4 h of equilibration, the aliquots of equilibrated solutions were filtered through a 0.2- μ m filter, and Hg concentrations were measured by CVAA.

Table 4.7. Experimental Conditions Used for Measuring the Distribution Coefficients

Constituent (mmol/L)	K1	K2
Iodide	90	90
Sulfate	88	88
K	265	265
Fe (II)	0.5	0.5
Ca	0.2	0.2
Hg	0.33	0.49

The results show that SAMMS material has very high selectivity (very high K_d values) for Hg in iodide-containing surrogate solutions (Table 4.8). The speciation calculations indicated

that in both solutions, HgI_4^{2-} species constituted about 92% of the total dissolved Hg, whereas HgI_3^- species formed a minor fraction (8%). When solutions containing 0.33 mmol/L of total Hg were contacted with SAMMS material, the equilibrium concentrations of Hg were below detection ($<5 \times 10^{-5}$ mg/L using CVAA). Consequently, the calculations show that SAMMS material has extremely high specificity ($K_d > 2.64 \times 10^8$ mL/g) for dissolved Hg (in HgI_4^{2-} and HgI_3^- complex forms) in the tested surrogate solution. The second set of duplicate experiments with solutions containing 0.49 mmol/L of Hg also showed that thiol-SAMMS material has very high specificities (K_d of 1.29×10^5 mL/g and 2.10×10^5 mL/g) for adsorbing anionic Hg-I complex species. The data obtained from these experiments indicate that thiol-SAMMS material, due to its very high selectivity (very high K_d and very low equilibrium Hg concentrations), can be used to remove soluble Hg from KI- K_2SO_4 waste-stream solutions.

Table 4.8. Distribution Coefficients for Adsorption of Hg by SAMMS Material from Surrogate Solutions

<u>Replicate</u>	<u>Initial Hg Conc. (mg/L)</u>	<u>Final Hg Conc. (mg/L)</u>	<u>Solid:Solution Ratio (g:mL)</u>	<u>K_d (mL/g)</u>
K1- 1	66	$<5 \times 10^{-5}$	1:200	$>2.64 \times 10^8$
K1-2	66	$<5 \times 10^{-5}$	1:200	$>2.64 \times 10^8$
K2-1	97.5	0.6	1:800	1.29×10^5
K2-2	97.5	0.4	1:800	2.10×10^5

5.0 Effects of Organic Ligands on Mercury Adsorption by Thiol-SAMMS

Ligands (organic and inorganic) that form strong complexes with dissolved Hg may affect the Hg-adsorption characteristics of SAMMS material. Strongly complexing ligands may be present in leachates from contaminated solid wastes and in liquid effluents. A previous study showed that the Hg-binding capability of thiol-SAMMS was reduced when strongly complexing inorganic ligands were present in equilibrating solutions (Feng et al. 1997b). However, data are lacking on the effects of organic ligands on Hg adsorption. The objective of this test is to examine the effects of such complexation on adsorption by using strongly complexing model ligands such as ammonia, EDTA (log $K = 21.5$ for Hg-EDTA complex), cyanide (log $K = 18$ for HgCN⁻ complex), and fulvate. Fulvate is a natural organic ligand that is commonly encountered in natural aqueous systems such as surface and ground waters. A set of tests was conducted to evaluate adsorption characteristics of thiol-SAMMS material with solutions containing 1:1 Hg-ligand complexes.

The experiments were conducted with solutions containing different concentrations of Hg and 0.5 mmol/L of respective ligands. Adsorption effects at three different pH (3, 7, and 9) values were evaluated. All experiments were conducted in duplicate at a fixed solution-solid ratio of about 120, and an equilibration time of 4 h. At the end of equilibration, the contacting solutions were filtered, and the filtrates were analyzed for Hg content using CVAA.

The adsorption data (Table 5.1) showed that compared to all other ligands, the naturally occurring organic ligand, fulvate had the most noticeable effect on Hg adsorption. Apparently, fulvate ligand by forming very strong complexes with Hg, affects Hg-adsorption affinity. However, the data also showed that 92 to 99% of Hg in fulvate solutions was adsorbed by thiol-SAMMS. These results suggested that thiol-SAMMS would adsorb significant amounts of Hg even when strongly complexing fulvate-like ligands are present in waste solutions. The very high affinity parameters (K_d values) indicated that the Hg complexes of ammonia, cyanide, and EDTA ligands had no noticeable effect on Hg binding by thiol-SAMMS. These data indicate that organic ligands that are similar to the model ligands, such as ammonia, cyanide, and EDTA, practically have no effect on Hg adsorption by thiol-SAMMS.

Table 5.1. Organic Ligand Effects on Hg Adsorption by thiol-SAMMS

Ligand	pH	Vol. of Solution (mL)	Wt. of SAMMS (mg)	Initial Hg Conc. (mg/L)	Final Hg Conc. (mg/L)	Hg adsorbed (mg/g)	Distribution Coefficient: K_d (mL/g)	Average K_d (mL/g)
NH ₃	3	20	165	46.7	0.0071	5.66	8.0E+05	
NH ₃	3	20	165	46.7	0.0074	5.66	7.7E+05	7.8E+05
NH ₃	7	20	165	1.3	0.0045	0.16	3.5E+04	
NH ₃	7	20	165	1.3	0.0033	0.16	4.8E+04	4.1E+04
NH ₃	9	20	165	1.5	0.0068	0.18	2.7E+04	
NH ₃	9	20	165	1.5	0.0027	0.18	6.8E+04	4.8E+04
CN	3	20	165	71.5	0.0150	8.66	5.8E+05	
CN	3	20	165	71.5	0.0080	8.67	1.1E+06	8.3E+05
CN	7	20	165	45.6	0.0089	5.53	6.2E+05	
CN	7	20	165	45.6	0.0032	5.53	1.7E+06	1.2E+06
CN	9	20	165	72.5	0.0034	8.79	2.6E+06	
CN	9	20	165	72.5	0.0027	8.79	3.3E+06	2.9E+06
EDTA	3	20	165	74.0	0.0060	8.97	1.5E+06	
EDTA	3	20	165	74.0	0.0070	8.97	1.3E+06	1.4E+06
EDTA	7	20	165	19.9	0.0045	2.41	5.4E+05	
EDTA	7	20	165	19.9	0.0043	2.41	5.6E+05	5.5E+05
EDTA	9	20	165	79.9	0.0041	9.68	2.4E+06	
EDTA	9	20	165	79.9	0.0049	9.68	2.0E+06	2.2E+06
FUL	3	20	165	55.3	0.7000	6.62	9.5E+03	
FUL	3	20	165	55.3	0.6200	6.63	1.1E+04	1.0E+04
FUL	7	20	165	59.0	5.6000	6.47	1.2E+03	
FUL	7	20	165	59.0	4.2000	6.64	1.6E+03	1.4E+03
FUL	9	20	165	60.9	3.1000	7.01	2.3E+03	
FUL	9	20	165	60.9	3.2000	6.99	2.2E+03	2.2E+03

6.0 Actinide Adsorption Characteristics of Functionalized SAMMS Material

Many DOE repositories contain various types of actinide-containing radioactive liquid wastes. Some of these wastes could be treated as low-level radioactive wastes if the actinides could be selectively removed. This would result in a substantial reduction of high-level radioactive waste volume, thereby significantly reducing the handling and disposal costs. Removal of actinides from high-level wastes is very challenging in that these wastes are usually complex salt solutions, containing high concentrations of nonradioactive cations that can compete with the actinides in binding to the sorbent materials. Previous studies have examined two processes, namely solvent extraction and ion exchange, for separating actinide elements from a highly complex solution matrix (Condamines and Musicas 1992; Maiti et al. 1992; Rozen et al. 1992; Horwitz et al. 1993, 1995; Karlova et al. 1994; Mathur et al. 1994). Due to the difficult nature of such separation processes, the sorbents used for this purpose must be structurally stable and exhibit very high selectivities for actinide ions. The objective of this investigation was to develop and demonstrate that SAMMS materials can be used in highly selective fashion to remove actinides from a matrix of a high concentration of salt solutions.

As indicated previously, SAMMS material can be designed to achieve high selectivity toward a specific class of cationic elements. As an example, actinide-specific SAMMS material has been developed by assembling certain actinide-binding ligands on synthetic mesoporous oxide substrates. (Harris et al. 1981; Riley et al. 1983; Scarrow et al. 1985a, b, 1988; Hou et al. 1994). In nature, it is known that siderophores use Lewis-base chelating groups, including catechols (e.g., enterobactin) and hydroxamic acids (e.g., desferrioxamine B). These chelating groups are often combined in polydentate ligands to fully bind the metal in a six-coordination complex. Raymond and coworkers made actinide sequestering agents by incorporating these chelating groups into multidentate ligands. They have also attached these ligands onto insoluble polymers for use as solid/liquid extractants (Whisenhunt 1994). Indices of affinity, the distribution coefficients, K_d , reported for thorium (IV) was as high as 70 mL/g for 1,2-HOPO and 250 mL/g for 3,4-HOPO resins at pH 5.8.

Mesoporous silica was synthesized in cetyltrimethylammonium chloride/hydroxide, silicate, and mesitylene solutions (Beck et al. 1992). The thiol-SAMMS was made by incorporating propylmercaptan onto the mesoporous materials as previously reported (Feng et al. 1997a). The probable molecular structure of thiol-SAMMS is shown in Figure 6.1. The HOPO-SAMMS was made by first incorporating a propylamine monolayer on the mesoporous materials through silinization methods similar to that of thiol-SAMMS. Elemental analysis of the amino-SAMMS found C, 15.73; H, 4.08; N, 5.45; Al, 1.61; Si, 11.00. Dimethylformamide was dried over molecular sieves (4 Å) and pyridine was dried over potassium hydroxide. All other reagents were purchased from commercial sources and used as received.

The 1,2-HOPO SAMMS was synthesized by dissolving 2.20 g (14.2 mmol) of 1,2-HOPO-6-carboxylic acid in 150 mL of dimethylformamide. A weighed quantity of (2.57 g) of 1, 1'-carbonyldiimidazole was stirred into this solution under nitrogen for 2 hours followed by

the addition of 2 g of amino-SAMMS. The mixture was stirred at room temperature for 4 days. The solution was filtered, and the solid product was washed with methanol and dried in a vacuum at 60°C overnight. This treatment resulted in about 2.43 g of an off-white powder. Elemental analysis of this compound indicated the composition to be C, 17.90; H, 3.91; N, 6.26; Si, 9.88; Al, 1.44. The probable molecular structure of 1,2-HOPO SAMMS is indicated in Figure 6.1.

The 3,4-HOPO SAMMS was synthesized by dissolving 5.87 g (27.1 mmol) of 3-benzyloxy-4-HOPO-N-methylearboxylic acid in 160 mL of pyridine. Weighed quantities (2.45 g) of N-hydroxysuccinimide and (4.40 g) of 1,3-dicyclohexylcarbodiimide were added to this solution, and the mixture was stirred overnight at room temperature. Next, about 4 g of amino-SAMMS were added, and the solution was stirred at room temperature under nitrogen for 4 days. The solution was filtered, and the resulting compound was washed with boiling tetrahydrofuran, distilled water, and methanol. The product was stirred for 2 days in 150 mL of a mixture of 1: 1 glacial acetic acid/concentrated hydrobromic Acid. The treated material was collected by filtration, washed with distilled water and methanol, and dried in vacuum at 60°C overnight, resulting in about 5.29 g of an off-white powder. Elemental analysis indicated the composition of this material to be C, 20.57; H, 4.75; N, 5.35; Al, 0.79; Si, 9.78. The probable molecular structure of 3,4-HOPO SAMMS is indicated in Figure 6.1.

For adsorption experiments, Am(III), Th(IV), Pu(IV), Np(V), Pu(VI), and U(VI) were selected as the models for tri-, tetra-, penta- and hexa-valent actinides, respectively. Background electrolyte for all experiments consisted of 0.1 M NaNO₃. The solutions were adjusted to different pH values with final equilibrium pH values ranging from 0.88 to 6.8. The adsorption tests were performed in batch mode using 20 mg of SAMMS powders in 5.0 mL of actinide-spiked 0.1 M NaNO₃ solutions. The solution-SAMMS mixtures were equilibrated at room temperature for 4 hours and filtered through 22- μ m filters, and the filtrates were analyzed for radionuclide activities. Liquid scintillation counting was used to measure ²⁴¹Am, ²³⁷Np, and ²³⁹Pu, and inductively coupled plasma-mass spectrometry (ICP-MS) was used to analyze ²³⁸U and ²³²Th.

The adsorption data (Table 6.1) showed that the 1,2-HOPO-SAMMS was very effective in removing Am (III) from solution. Adsorption by 1,2-HOPO-SAMMS at a pH of 6.8 reduced concentrations of ²¹¹Am from 7.1 μ g/L to 4 ng/L (activity reduced from 53,500 cpm/mL to 30 cpm/mL). The affinity parameter, K_d was calculated to be in the range of 1.9×10^5 mL/g at pH 0.88 to 4.5×10^5 mL/g at pH 6.8. Thiol-SAMMS had a lower affinity (K_d values 449 to 6190 mL/g) for Am (III) as compared to 1,2-HOPO. Among the SAMMS tested, the 3,4-HOPO-SAMMS showed the lowest affinity for binding Am(III). These data were confirmed by a previous study of Am (III) adsorption onto 60 selected commercial and laboratory absorbers in which the the highest K_d value under acidic conditions was 9.4 mL/g (Marsh et al., 1993).

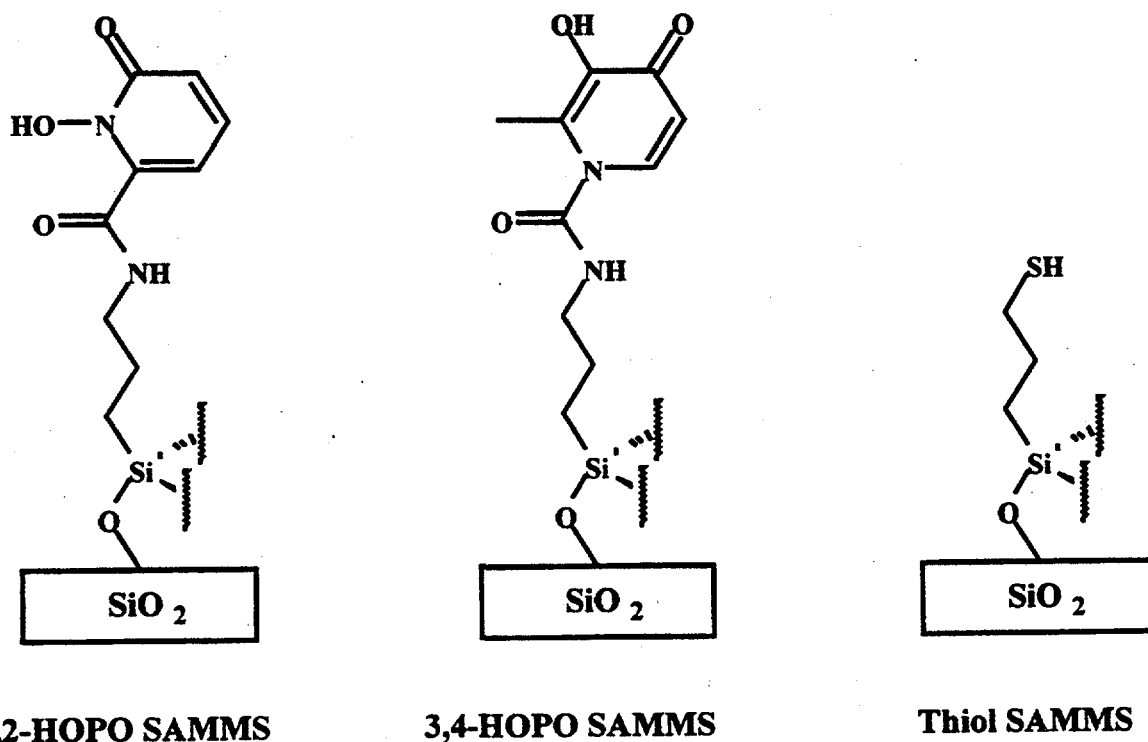


Figure 6.1. Molecular Structures of 1,2-HOPO-SAMMS, 3,4-HOPO-SAMMS, and thiol-SAMMS

The data showed that all the adsorbents tested (thiol-SAMMS, 1,2-HOPO-SAMMS, and 3,4-HOPO-SAMMS) have only moderate affinities (K_d in the range of 160 mL/g at pH 0.88 and 841 mL/g at pH 3) for adsorbing Th(IV) from solution. By contrast, thiol-SAMMS exhibited greater affinity (K_d , 1660 mL/g) for bonding another tetravalent actinide namely, Pu(IV).

Among the adsorbents tested, only 1,2-HOPO-SAMMS showed more specificity for binding Np(V). The selectivity coefficients (K_d values of 195, 425, 3260, and 3630 mL/g at pH values of 0.88, 3.2, 5.6, and 6.30, respectively) indicated significantly enhanced affinity of 1,2-HOPO-SAMMS for binding Np(V) at higher pH values.

The data for adsorption of hexavalent actinides indicated that thiol-SAMMS had a very high preference (K_d , >10000 mL/g) for adsorbing Pu(VI). This selectivity value is at least an order of magnitude higher than any previously reported data (highest K_d , 2185 mL/g) for Pu(IV) adsorption on 60 different commercial and laboratory adsorbents (Marsh et al. 1993). By comparison, the 1,2-HOPO-SAMMS showed only moderate binding affinities for another hexavalent actinide namely, U(VI) with K_d values ranging from 180 mL/g at pH 0.88 to 620 mL/g at pH 3.0. Two other adsorbents, thiol-SAMMS and 3,4-HOPO-SAMMS, exhibited significantly lower binding affinities (<75 mL/g) than 1,2-HOPO-SAMMS for U(VI) adsorption.

It is important to note that for Th(IV) adsorption, the 1,2-HOPO-SAMMS showed higher affinity (K_d , 840 mL/g) than the HOPO resins (K_d , 70 mL/g). Even the thiol-SAMMS material showed higher affinity for Th(IV) as compared to the adsorption performance of thiol-resins. However, the 3,4-HOPO-SAMMS material showed lower affinity (K_d , 114 mL/g) for Th

(IV) adsorption than did the corresponding 3,4-HOPO resin form (K_d , 260 mL/g). At this point, it is still not clear why the 1,2-HOPO-SAMMS behaves so differently than the 3,4-HOPO-SAMMS in its actinide adsorption affinities, while there are no significant differences in actinide binding behavior between resin forms of 1,2-HOPO and 3,4-HOPO. The complex structures of these functional groups in the resins and in the SAMMS substrates will have to be studied in greater detail to provide an improved understanding about the observed differences in their actinide-adsorption affinities.

Table 6.1. Actinide Absorption on Functionalized SAMMS

<u>Element</u>	<u>Vol</u> <u>mL</u>	<u>SAMMS</u> <u>g</u>	<u>pH</u>	<u>Final</u> <u>cpm/mL</u>	<u>Initial</u> <u>cpm/mL</u>	<u>Final</u> <u>µg/L</u>	<u>Initial</u> <u>µg/L</u>	<u>K_d</u> <u>(mL/g)</u>
1,2-HOPO-SAMMS								
Am(III)	5	0.02	0.88	390	302000	0.051	39.8	194850
Am(III)	5	0.02	4.50	28	24200	0.004	3.2	199750
Am(III)	5	0.02	6.80	30	53500	0.004	7.1	443500
Np(V)	5	0.02	0.88	41300	73400	26993	48000	195
Np(V)	5	0.02	3.20	27200	73400	17778	48000	425
Np(V)	5	0.02	5.60	5140	72200	3359	47200	3260
Np(V)	5	0.02	6.30	4450	69000	2908	45100	3630
Th(IV)	5	0.02	0.82			86300	141400	160
Th(IV)	5	0.02	3.40			30500	133100	841
U(VI)	5	0.02	0.85			78500	135400	181
U(VI)	5	0.02	3.00			39400	136800	618
Thiol-SAMMS								
Am(III)	5	0.02	0.84	108000	302000	14.248	39.8	449
Am(III)	5	0.02	3.10	17500	296000	2.309	39.1	3980
Am(III)	5	0.02	3.70	11300	291000	1.491	38.4	6190
Np(V)	5	0.02	0.84	67900	70500	44379	46100	9.69
Np(V)	5	0.02	3.10	67900	70400	44379	46000	9.13
Th(IV)	5	0.02	0.87			86800	141400	157
Th(IV)	5	0.02	3.00			53800	133100	368
U(VI)	5	0.02	0.85			132600	135400	5.28
U(VI)	5	0.02	3.00			105700	136800	73.6
Pu(IV)	5	0.10	1.00	350	12000			1660
Pu(VI)	5	0.10	3.00	backgd	8000			> 10000
3,4-HOPO-SAMMS								
Am(III)	5	0.02	0.84	292000	302000	38.522	39.8	8.56
Am(III)	5	0.02	2.60	288000	296000	37.995	39.1	6.94
Np(V)	5	0.02	0.75	69700	70500	45556	46100	2.99
Np(V)	5	0.02	2.50	69500	70400	45425	46000	3.16
Th(IV)	5	0.02	0.84			109000	141400	74.3
Th(IV)	5	0.02	2.60			91500	133100	114
U(VI)	5	0.02	0.86			130000	135400	10.4
U(VI)	5	0.02	2.60			105400	136800	74.5

This preliminary study showed that by incorporating actinide-specific functional groups, such as 1,2-hydroxypyridinone, into SAMMS substrates, an effective scavenger for actinides can be produced. These SAMMS-based adsorbents are very effective in removing tri-, tetra-, penta-, and hexa-valent actinides from salt solutions. The thiol-SAMMS, however, is only effective for removing tri-, tetra- and hexa-valent actinide forms. In contrast, the 3,4-HOPO-SAMMS is not very effective for separating actinides from a salt-solution matrix. Incorporating functional groups such as catechol into a SAMMS substrate may result in even better actinide-removing sorbents because previous studies by Raymond and his coworkers have shown that a catechol resin is almost three times more effective in removing Th(IV) than the corresponding 1,2-HOPO- and 3,4-HOPO resins.

7.0 Transition Metal Adsorption Characteristics of Thiol- SAMMS

Mesoporous silica materials functionalized with thiol functional groups (thiol-SAMMS) were designed to specifically adsorb Hg from various types of waste solutions. Previous studies on different types of Hg-containing aqueous and non-aqueous solutions have established the range of Hg-loading and affinity characteristics for thiol-SAMMS material (Feng et al. 1997b; Mattigod et al. 1997b). These studies also showed that thiol-SAMMS can specifically adsorb Hg from solutions that contain competing transition-metal cations. These previous experiments also indicated that thiol-SAMMS may also adsorb other soft cations that belong to various transition-metal series. Therefore, the objective of this investigation was to examine the affinity of thiol-SAMMS material for adsorbing some common transition metals.

Adsorption Experiments were conducted using about 0.1 g thiol-SAMMS material in 10 mL of 0.1 M NaNO₃ solution containing selected metals. After equilibration, the metal concentrations were measured in the filtrate, and the affinity parameter was calculated. The adsorption tests included selected transition metals, such as Ag, Cd, Co, Cr, Cu, Eu, and Zn. For comparative purposes, two alkaline earth elements, Ca and Mg, and a toxic metal, Pb, were also tested .

The results (Table 8.1) showed that thiol-SAMMS has very high affinities for adsorbing soft cations such as Ag, Cd, Cu(II), Cr(III), and Pb. These data confirm the high specificity of the soft-base thiol groups for adsorbing soft acid cations. The data also showed that thiol-SAMMS does not show any affinity for adsorbing alkaline-earth elements and very low affinity for Co(II) and Zn.

These results suggest that thiol-SAMMS, even in the presence of alkali and alkaline-earth cations, can adsorb, in addition to Hg, other soft acid cations (Ag, Cd, Cu(II), Cr(III), and Pb). Additional studies are needed to elucidate the relationship between the degree of cation softness (such as Misono Softness Parameter) and the adsorption affinity (K_d values) of thiol-SAMMS.

Table 7.1. Binding Affinity of Thiol-SAMMS for Selected Metal Species

Metal	Ini. Conc. µg/L	Final Conc µg/L	K_d (mL/g)
Ag(I)	90	10	8900
Ca(II)	2070	2070	0
Cd(II)	4670	32	14467
Co(II)	2810	2670	5
Cr(III)	2630	20	700
Eu(III)	9010	1220	639
Cu(II)	2240	<5	>44700
Pb(II)	3040	300	913
Mg(II)	1580	1580	0
Zn(II)	2790	2410	16

8.0 Conclusions

The following conclusions can be made from the experiments conducted and described.

8.1 Mercury-Adsorption Kinetics and Loading Capacity of Thiol-SAMMS

- Aqueous-speciation calculations indicated that a major fraction (92 to 99%) of dissolved Hg in KI-K₂SO₄ waste solution exists in the form of HgI₄²⁻; therefore, adsorption of Hg by thiol-SAMMS would be controlled mainly by the concentration (activity) of this species.
- The kinetics data showed that at all pH values (3, 5, 7, and 9), Hg adsorption by thiol-SAMMS occurred very rapidly (~ 82 to 95% of total Hg adsorption occurred within the first 5 min). In all cases, the adsorption equilibrium was attained within ~4 h.
- The loading-density measurements showed that at fixed solid:solution ratio, the loading density increased with decreasing iodide concentrations. The highest Hg loading of ~270 mg/g of thiol-SAMMS was observed at ~90 mmol/L iodide concentration.
- Free energy of adsorption data indicated that Hg²⁺ ion has high affinity for thiol-groups attached to the mesoporous silica material. This strong adsorption affinity is typical of soft-cation/soft-base interaction.
- Very high distribution-coefficient values (K_d , 1.2910⁵ to >2.64 × 10⁸) confirm that thiol-SAMMS adsorbs Hg from KI-K₂SO₄ solutions with very high specificity.

8.2 Effects of Organic ligands on Hg Adsorption by Thiol-SAMMS

- Very-high-affinity parameters indicated that ligands, ammonia, cyanide, and EDTA had no effect on Hg adsorption by thiol-SAMMS.
- In the presence of a strongly complexing ligand (fulvate), thiol-SAMMS removed ~92 to 99% of Hg in solution.

8.3 Actinide Adsorption Characteristics of Functionalized SAMMS Material

- 1,2-HOPO-SAMMS had a very high affinity (K_d : 1.9 × 10⁵ to 4.43 × 10⁵ mL/g) for Am(III), a high affinity (K_d : 3.3 × 10³ to 3.6 × 10³ mL/g) for Np(V), and moderate affinities (K_d : 160 to 840 mL/g) for Th(IV) and U(VI).
- Thiol-SAMMS showed a very high affinity (K_d : >1.0 × 10⁴ mL/g) for Pu(VI) and high affinities (K_d : 4.0 × 10³ to 6.2 × 10³ mL/g) for Am(III) and Pu(IV) (K_d : 1.7 × 10³ mL/g).
- 1,2-HOPO-SAMMS and thiol-SAMMS were significantly more effective than resin forms for adsorbing actinides.

8.4 Transition Metal Adsorption Characteristics of Thiol-SAMMS

- Thiol-SAMMS showed high affinities for adsorbing soft cations, such as Ag, Cd, Cu(II), Cr(III), and Pb. These data confirmed the high specificity of soft-base thiol groups for adsorbing soft-acid cations.
- Due to its high specificity, thiol SAMMS can selectively adsorb and separate Ag, Cd, Cu(II), Cr(III), Hg, and Pb from solutions containing alkali and alkaline-earth cations.

9.0 References

- Beck, J. S., J. C. Vartuli, W. J. Roth, M. E. Leonowicz, C. T. Kresge, K. D. Schmitt, C. T. W. Chu, D. H. Olson, E. W. Sheppard, S. B. McCullen, J. B. Higgins, J. L. Schlenker. 1992. "A new family of mesoporous molecular sieves prepared with liquid crystal templates." *J. Am. Chem. Soc.* 114:10834.
- Bishop, A. R., and R. G. Nuzzo. 1996. "Self-Assembled Monolayers, Recent Developments and Applications," *Cur. Opin. Colloidal & Inter. Sci.* 1:127.
- Bunker, B. C., P. C. Rieke, B. J. Tarasevitch, A. A. Campbell, G. E. Fryxell, G. L. Graff, L. Song, J. Liu, and J. W. Virden. 1994. "Ceramic thin film formation on functionalist interfaces through biomimetic processing." *Science.* 264:48-55.
- Condamines, N., and C. Musikas. 1992. "The Extraction by N,N-Dialkylamides. 2. Extraction of Actinide Cations," *Solv. Extr. Ion Exch.* 10(1):69-100.
- Dyrssen, D., D. Jagner, and, F. Wengelin. 1968. *Computer Calculation of Ionic Equilibria and Titration Procedures.* Almquist and Wiksell, Stockholm, Sweden.
- Feng, X., G. E. Fryxell, L.-Q. Wang, A. Y. Kim, J. Liu, and K. M. Kemner. 1997a. "Functionalized Monolayers on Ordered Mesoporous Supports (SAMMS)," *Science.* 276:913-926.
- Feng, X., J. Liu, G. E. Fryxell, M. Gong, L. Wang, D. E. Kurath, C. S. Ghormley, K. T. Klasson, and K. M. Kemner. 1997b. *Self-Assembled Mercaptan on Mesoporous Silica (SAMMS) for Mercury removal and stabilization*, PNNL-11691, Pacific Northwest National Laboratory, Richland, Washington.
- Foust, D.F. 1993. *Extraction of Mercury and Mercury Compounds from Contaminated Material and Solutions.* US Patent 5,226,545.
- Ghazy, S. E., "Removal of Cadmium, Lead, Mercury, Tin, Antimony, and Arsenic from Drinking and Seawaters by Colloid Precipitate Flotation," *Sep. Sci. Technol.* 30(6):933(1995).
- Greenberg, S. A., and, L. E. Copeland. 1960. "Thermodynamic Functions for the Solution of Calcium hydroxide in Water." *J. Phy. Chem.* 64:1057-1059.
- Harris, W. R., K. N. Raymond, and F. L. Weigl. 1981. "Ferric Ion Sequestering Agents. 6. The Spectrophotometric and Potentiometric Evaluation of Sulfanated Tricatecholate Ligands." *J. Am. Chem. Soc.* 103:2667.
- Horwitz, E. P., R. Chiarizia, H. Diamond, and R.C. Gatrone. 1993. "Uptake of Metal Ions by A New Chelating Ion-Exchange Resin. 1. Acid Dependencies of Actinide Ions," *Solv. Ion Exch.* 11(5):943-966.

- Horwitz, E. P., M. L. Dietz, R. Chiarizia, and H. Dimond. 1995. "Separation and Preconcentration of Actinides by Extraction Chromatography Using A Supported Liquid Anion Exchanger - Application to the Characterization of High-level Nuclear Waste Solutions," *Analytica Chimica Acta*. 310(1):63-78.
- Hou, Z., D. W. Whisenhunt, Jr., J. Xu, and K. N. Raymond. 1994. "Potentiometric and ^1H NMR Study of Four Desferrioxamine B Derivatives and Their Ferric Complexes." *J. Am. Chem. Soc.* 116:840.
- Karalova, Z. K., E. A. Lavrinovich, B. F. Myasoedov, and L. A. Fedorov. 1994. "Extraction of Actinides and Lanthanides by Alkylphenol Sulfides." *Radiochemistry*. 36(5):441-445.
- Kresge, C. T., M. E. Leonowicz, W. J. Roth, J. C. Vartuli, and J. S. Beck. 1992. "Ordered mesoporous molecular sieves synthesized by a liquid crystal template mechanism." *Nature*. 359:710-712.
- Larson, K. A., and J. M. Wiencek. 1994. "Mercury Removal from Aqueous Streams Utilizing Microemulsion Liquid Membranes." *Environ. Prog.* 13(4):253.
- Liu, J., A. Y. Kim, J. Virden, and B. C. Bunker. 1995. "Preparation of mesoporous spherulite in surfactant solutions." *J. Porous Mater.* 2:201-205.
- Liu, J., A. Y. Kim, L. Q. Wang, B. J. Palmer, Y. L. Chen, P. Bruinsma, B. C. Bunker, G. J. Exarhos, G. L. Graff, P. C. Rieke, G. E. Fryxell, J. W. Virden, B. J. Tarasevich, and L. A. Chick. 1996a. "Self-Assembly in Materials Synthesis," invited review article, *Adv. Colloidal Inter. Sci.* 69:131-180.
- Liu, J., A. Y. Kim, J. Virden, B. C. Bunker. 1996b. "Effect of colloidal particles on the formation of ordered mesoporous materials." *Langmuir*. 11:689-692.
- Liu, J., X. Feng, G. E. Fryxell, L- Q. Wang, A. Y. Kim, and M. Gong. 1998. "Hybrid Mesoporous Materials with Functionalized Monolayers." *Adv. Mater.* 10:161-165.
- Maiti, T. C., J. H. Kaye, A. E. Kozelisky. 1992. "Sequential Separation of Pu, Np, U, and Am from Highly Radioactive Hanford Waste by Ion Exchange Methods," *J. Radioanal. Nucl. Chem.-Art.* 161(2):533-540.
- Marsh, S. F., Z. V. Svitra, and S. M. Bowen. 1993. Los Alamos National Laboratory Report LA 12654, Los Alamos, New Mexico.
- Martell, A. E., and R. N. Smith. 1982. *Critical Stability Constants. V5, I Supplement*. Plenum Press, New York.
- Mathur, J. N., M. S. Murali, G. H. Rizvi, and R. H. Iyer. 1994. "Separation and Recovery of Plutonium from Oxalate Supernatant Using CMPO." *Solv. Extr. Ion Exch.* 12(4):745-763.
- Mattigod, S. V., and G. Sposito. 1977. "Estimated Association Constants of Some Complexes of Trace Metals With Inorganic Ligands." *Soil Sci. Soc. Am. J.* 41:1092-1097.

Mattigod, S. V., and G. Sposito. 1979. "Chemical Modeling of Trace Metal Equilibria in Contaminated Soil Solutions Using the Computer Program GEOCHEM." *In Chemical Modeling in Aqueous Systems*. Ed. E. A. Jenne. ACS Sym. Ser 93. American Chemical Society, Washington D.C.

Mattigod, S. V. 1996. "Validation of Geochemical Equilibrium Models." *In Chemical Equilibrium and Reaction Models*. Soil Science Society of America, Madison, Wisconsin.

Mattigod, S. V., and J. M. Zachara. 1997a. "Equilibrium Modeling in Soil Chemistry." *In Methods of Soil Analysis Part 3 Chemical Methods*, Soil Science Society of America, Madison, Wisconsin.

Mattigod, S. V., Feng, X., G. E. Fryxell, J. Liu, M. Gong, C. S. Ghormley, S. Baskaran, Z. Nie and K. T. Klasson. 1997b. *Mercury Separation from Concentrated Potassium Iodide/Iodine Leachate Using Self-Assembled Mercaptan on Mesoporous Silica (SAMMS) Technology*, PNNL-11714, Pacific Northwest National Laboratory, Richland, Washington.

Mitra, S. 1986. *Mercury in the Ecosystem*. Trans. Tech. Publications, Lancaster, Pennsylvania.

Nieboer, E., and A. E. McBryde. 1973. "Free-Energy Relationships in Coordination Chemistry. III A Comprehensive Index to Complex Stability." *Can. J. Chem.* 51:2512-2524.

Otani, Y., H. Emi, C. Kanaoka, and H. Nishino. 1988. "Removal of Mercury Vapor from Air with Sulfur-Impregnated Adsorbents," *Environ. Sci. Technol.* 22(6), 708.

Riley, P. E., K. Abu-Dari, and K. N. Raymond. 1983. "Specific Sequestering Agents for the actinides. 9. Synthesis of Metal Complexes of 1-Hydroxy-2-Pyridinone and the Crystal Structure of Tetrakis(1-oxy-2-pyridonato) aquothorium (IV) Dihydrate." *Inorg. Chem.* 22:3940.

Ritter, J. A., and J. P. Bibler. 1992. Toxic Waste Management in the Chemical and Petrochemical Industries. "Removal of Mercury From Waste Water: Large-scale Performance of An Ion Exchange Process," *Water Sci. Technol.* 25(3):165.

Rozen, A. M., A. S. Nikiforov, B. S. Zakharkin, Z. I. Nikolotova. 1992. "Optimized Extracting Agents for Removal Actinides." *Atomnaya Energiya.* 72(5):453-459.

Scarrow, R. C., P. E. Riley, K. Abu-Dari, D. L. White, and K. N. Raymond. 1985. "Ferric Ion Sequestering Agents. 13. Synthesis, Structures and Thermodynamics of Complexation of Cobalt(III) and Iron(III) Tris Complexes of several Chelating Hydroxypyridinones." *Inorg. Chem.* 24:954.

Scarrow, R. C., P. E. Riley, D. L. White, and K. N. Raymond. 1985. "Ferric Ion Sequestering Agents, 14. 1-Hydroxy-2(1H)-pyridinon Complexes: Properties and Structure of a Novel Fe-Fe Dimer," *J. Am. Chem. Soc.* 107:6540.

Scarrow, R. C., and K. N. Raymond. 1988. "Synthesis of N-Alkyl-3-hydroxy-2(1H)-Pyridinones and Coordination Complexes with Iron(III)," *Inorg. Chem.* 27:4140.

- Smith, R. N., and A.E. Martell. 1976. *Critical Stability Constants*. V4. Plenum Press, New York.
- Smith, R. N., and A. E. Martell. 1989. *Critical Stability Constants*. V6, II Supplement. Plenum Press, New York.
- U.S. Department of Energy (DOE). 1991. "FY91 Waste and Hazard Minimization Accomplishments," USDOE Report MHSMP-91-37, Pantex Plant, Amarillo, Texas.
- U.S. Department of Energy (DOE). 1996. Mixed Waste Focus Area, "Technical Baseline Results," World Web: [Http://wastenot.inel.gov/mwfa/results.html](http://wastenot.inel.gov/mwfa/results.html).
- Wagman, D. D., W. H. Evans, V. B. Parker, I. Halow, S. M. Bailey, and H. Schumm. 1969. "Selected Values of Chemical Thermodynamic Properties," *Nat. Bur. Stand. Tech. Notes*. 270:5.
- Whisenhunt, D. W., Jr. 1994. Synthesis and Evaluation of Chelating Agents and Resins Specific for the Actinides, Ph.D. Thesis, University of California at Berkeley.
- Whitesides, G. M. 1996. "Self-Assembled Materials," *Scientific American*. September:146.

Appendix A

Awards, Publications, and Press Highlights

Appendix A: Awards, Presentations, and Press Highlights

Awards

- PNNL Self Assembled Monolayers on Mesoporous Supports (SAMMS) technology received the prestigious R&D 100 Award for 1998.
- SAMMS Technology was selected as a finalist in Technology Innovation category for the Discover Magazine Award.

Publications

- Liu, J. et al. 1998. "Hybrid Mesoporous Materials with Functionalized Monolayers." *Adv. Mater.*, 10:161-165.
- Liu J., et al. 1998. "Hybrid Mesoporous Materials with Functionalized Monolayers." *Chem. Eng. Tech.*, 21:96-100.

Press Highlights

- **Environmental Health Perspectives in 1998** featured SAMMS technology in a feature article entitled "Quick fixes for Quick Silver," 106:A74-A76.

Distribution

<u>No. of Copies</u>		<u>No. of Copies</u>	
	OFFSITE		OFFSITE
12	<p>DOE/Office of Scientific and Technical Information</p> <p>Greg Hulet Lockheed Martin Idaho Technologies Co. PO Box 1625 Idaho Falls, ID 83415-3875</p> <p>Dirk Gombert Lockheed Martin Idaho Technologies Co. PO Box 1625 Idaho Falls, ID 83415</p> <p>Jay Roach Lockheed Martin Idaho Technologies Co. PO Box 1625 Idaho Falls, ID 83415</p> <p>John Mathur U.S. Department of Energy Office of Science and Technology Germantown, MD 29874</p> <p>Jerry L. Harness U.S. Department of Energy 3 Main Street Oak Ridge, Tennessee 37830-8620</p> <p>Jack S. Watson Oak Ridge National Laboratory P.O. Box 2008 Oak Ridge, TN 37831</p> <p>K. T. Klasson Oak Ridge National Laboratory P.O. Box 2008 Oak Ridge, TN 37831</p>		<p>Tom Conley Oak Ridge National Laboratory P.O. Box 2008 Oak Ridge, TN 37831</p> <p>M. J. Steindler Argonne National Laboratory Bldg. 205 9700 S. Cass Avenue Argonne, IL 60439-4837</p> <p>J. C. Cunnane Argonne National Laboratory Bldg.2059700 S. Cass Avenue Argonne, IL 60439-4837</p> <p>M. C. Thompson Westinghouse Savannah River Co. Savannah River Technology Center P.O. Box 616 Aiken, SC 29802</p> <p>T. M. Kafka 3M Center, Bldg. 209-1W-24 St. Paul, MN 55144-1000</p> <p>S. L. Stein Greenhill Technologies PO BOX 5395, 4000 NE 41st St. Seattle, WA 98105-5428</p> <p>P. J. Usinowicz 505 King Avenue Columbus, Ohio 43201-2693</p>

No. of
Copies

OFFSITE

W.C. MacDonald
505 King Avenue
Columbus, Ohio 43201-2693

S. Cohen
505 King Avenue
Columbus, Ohio 43201-2693

W.W. Simmons
505 King Avenue
Columbus, Ohio 43201-2693
N. K. Chung
Metcalf & Eddy
30 Harvard Mill Square
PO Box 4071
Wakefield, MA 01880-5371

Ken M. Kemner
Argonne National Laboratory
9700 S. Cass Ave.
Argonne, IL 60439

No. of
Copies

ONSITE

4 **DOE Richland Operations Office**

T. L. Aldridge, K8-50
R.A. Pressentin, K8-50
S.N Saget, K8-50
D. A. Brown, K8-50

52 **Pacific Northwest Laboratory**

S. Baskaran, K2-44
Bill Bonner, K9-14
B. C. Bunker, K2-45
Jim Buelt, P7-41
G. E. Fryxell, K2-44
M. Gong, P7-41
Bill Kuhn, K8-93
Jun Liu, K2-44 (25)
Nick Lombardo (6)
S. V. Mattigod, K6-81(2)
Z. Nie, K2-44
Joe Perez, P7-41
John Sealock, K2-10
Terri Stewart, K9-69
Rod Quinn, K9-69
Jud Virden, K2-44
L-Q. Wang, K2-44
Technical Report Files (5)